Review

Recent Progression and Opportunities of Polysaccharide Assisted Bio-Electrolyte Membranes for Rechargeable Charge Storage and Conversion Devices

Perumal Pandurangan [1,2]

1   Department of Hydro and Electrometallurgy, CSIR-Institute of Minerals and Materials Technology, Bhubaneswar 750103, Odisha, India; perumal@bgu.ac.il
2   Department of Materials Engineering, Ben-Gurion University of the Negev, Beersheva 84105, Israel

Abstract: Polysaccharide-based natural polymer electrolyte membranes have had tremendous consideration for the various energy storage operations including wearable electronic and hybrid vehicle industries, due to their unique and predominant qualities. Furthermore, they have fascinating oxygen functionality results of a higher flexible nature and help to form easier coordination of metal ions thus improving the conducting profiles of polymer electrolytes. Mixed operations of the various alkali and alkaline metal–salt-incorporated biopolymer electrolytes based on different polysaccharide materials and their charge transportation mechanisms are detailly explained in the review. Furthermore, recent developments in polysaccharide electrolyte separators and their important electrochemical findings are discussed and highlighted. Notably, the characteristics and ion-conducting mechanisms of different biopolymer electrolytes are reviewed in depth here. Finally, the overall conclusion and mandatory conditions that are required to implement biopolymer electrolytes as a potential candidate for the next generation of clean/green flexible bio-energy devices with enhanced safety; several future perspectives are also discussed and suggested.

1. Introduction

Nowadays, electrochemical devices and portable electronic appliances have received an extraordinary place in everyday lifestyles and it is difficult to think of the globe without the participation of the same types of devices [1]. Normally, an electrochemical device consists of three fundamental functional components such as an anode (negative electrode), electrolyte, and cathode (positive electrode), in which the electrolyte part plays a more important role than that of the electrode. Since electrolytes are executing the role of ion transmission between electrodes and also help to achieve superior electrochemical performance in terms of energy density and time stability of the device [1–3]. Even though popular electrical storage/conversion devices contain liquid electrolytes for the ion transfer process. The employment of liquid electrolyte systems is not encouraged for higher energy density applications, due to their insufficient electrochemical performance. In addition, it has some immature issues such as leakage of electrolytes, the reaction among electrodes, short circuits, lesser thermal stability, narrow window stability, and low safety. Hence, various strategies have been established to improve the electrolyte properties via the development of novel electrolyte systems and incorporation of additives without compromising the conducting properties.

With this approach, the replacement of liquid with solid electrolytes is very much appreciable and attractive as an alternative. The advantage of a solid system is the absence of leakage, wider electrochemical stability window, absence of volatility, etc. Thus, it helps to accomplish excellent charge storage performance and prevents short circuits of the

device thereby improving the safety parameter of the storage device [1–5]. Normally, solid electrolytes (SEs) are majorly divided into two types: (i) solid ceramic/nano electrolytes and (ii) polymer electrolytes.

At first, solid ceramic/nano electrolytes exhibit the appropriate properties including higher ionic conductivity, safety, and thermal stability. Unfortunately, the experimental and synthesis condition of the same is hard-hitting when compared to other SE preparation. Notably, the ceramic electrolyte system demonstrates poorer structural flexibility than that of polymer solid electrolytes. Based on the structural arrangements and framework of the materials, solid ceramic electrolytes contain minor classifications, too, which include Perovskite, LASICON, NASICON, garnet, etc. [6,7]. Thriving review articles on the conceptualization and ion-conducting mechanisms of the aforementioned ceramic electrolytes are available nowadays [7,8]. Nonetheless, the adaptation of polymer electrolytes (PEs) is discussed further in this article for the variety of electrochemical applications.

The potential selectivity of PEs is a highly admirable candidate in the wearable electronic industries, owing to its flexible and lightweight nature. As a result of this, it is possible to formulate direct stacking of the device in a single package, which leads to attaining higher operating voltage thereby reduction in the volume of the cell. These are more favorable parameters for higher energy density applications including electric vehicles (EVs), hybrid electric vehicles (HEVs), grid storage, and storage of wind and solar [9,10]. A study on polymer electrolytes was first initiated by P.V. Wright and co-workers [11] in 1971 and followed by various research groups. Polymer electrolytes are further classified into three categories like solid, gel, and composite PEs. Over the past decades, the development of synthetic PEs has gained significant attention from global researchers not only for the secondary battery system and also for other electrochemical applications including supercapacitors, solar cells, fuel cells, and electrochromic devices, etc. However, it can be a good material for electrical operations but its non-degradable and non-renewable nature makes it inappropriate for longer life purposes and causes environmental hazards because synthetic polymer products are extracted from the petrochemical source [12,13].

In modern times, environmental problems, including earth warming and ecological toxicity, are special challenging issues, due to CO_2 emission, and the generation of greenhouse gases. Therefore, the adaptation of natural materials and biomaterials is one of the choices to solve the existing environmental troubles at the same time as promoting sustainable energy and technology. From the greener viewpoint, degradable or natural resources are welcoming candidates and are believed to be a good substitute material for petroleum-derived synthetic products [3–13]. Since these compounds are extracted from the bio-materials and are in the organic carbon cycle through their decomposition process. Furthermore, studies on biopolymer materials have proved that they have low production costs when compared to polyethylene- and polypropylene-based synthetic electrolyte separators. In short, the advantage of natural polymer is being bio-compatible, renewable, recyclable, carbon neutral, eco-friendly, water-soluble, having good adhesive properties, etc. The changes in the physical and chemical properties of natural polymers and improvement in their functional characteristics have been performed via various chemical reactions, which contain etherification, esterification, grafting, and cross-linking whereas plasticization comes under the physical process [14]. Biopolymers are classified mainly into three types such as polynucleotides, polypeptides, and polysaccharides. Polynucleotides (RNA and DNA) are the longer type of polymers and are made of 13 or more than 13 nucleotide monomers. Second, polypeptides are short polymers and are classified under the category of amino acids. Finally, polysaccharides are linearly linked polymeric carbohydrate structures [15].

The structure of polysaccharides is composed of more than two monosaccharide entities joined together via glycosidic linkages with the condensation reaction, resulting in a larger structure and higher molecular weight [15]. For instance, starch, glycogen, cellulose, chitin, pectin, and tamarind seed polysaccharides are the majorly utilized biomaterials in the cluster of polysaccharide compounds. Interesting to note that, polysaccharide-based

biomaterials are of great interest in several fields such as drug delivery, tissue engineering, wound healing, pharmaceutical, food additives, etc. [14]. Moreover, the potential use of biopolymers in electrochemical applications is quite interesting and also served as an alternate candidate for the synthetic source with improved safety and eco-friendliness. The advantages of polysaccharides and their applications are pictorially given in Figure 1.
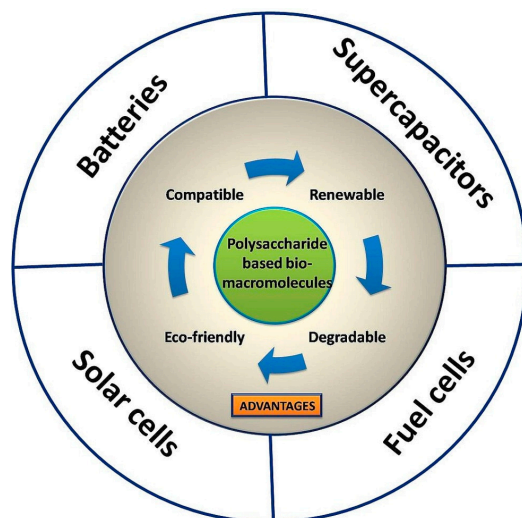

Figure 1. Advantages and applications of the polysaccharide compounds in electrical systems.

Noteworthy, classification, desirable properties, and ideal criteria for the selection of polymer host have been elaborately reported in the various earlier reviews [2,5,12,13,16]. From the vast discussion of the literature survey, there is not much attention and interest dedicated to discussing the overview of the polysaccharide-based biopolymer electrolytes. Hence, this review article discusses and represents the mixing operations of bio-electrical devices with the use of polysaccharide-based electrolytes. Interestingly, this is the first review article based on polysaccharide compounds and their present developments towards various electrochemical applications including lithium polymer/solid-state batteries, super capacitors, proton exchange membrane fuel cells, direct methanol fuel cells, solar cells, and magnesium ion batteries. Along with this, enrichment in the ionic conductivity of the membranes and corresponding contributing factors is elaborately highlighted. Finally, a summary of the present review theme and future outlook is suggested and discussed.

2. Ion Transport Mechanisms in the Polymer Electrolytes

Polymer hosts consist of several functional groups on their backbone such as hydroxyl, carbonyl, OSO^-, COO^-, etc. These oxygenated functional groups have a higher tendency to act as electron donors, due to their higher value of electro-negativity [3,17,18]. Therefore, incorporated alkali/alkaline metal salts have been dissociated into corresponding cations/anions and polymer backbone has a higher ability to form a coordination bond with metal cations, owing to their higher dielectric constant. The simple mathematical representation for this coordination process is written as follows,

$$B + MX \rightarrow BM^+ + X^- \tag{1}$$
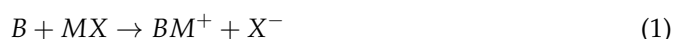
where *B*—biopolymer host, *MX*—doped alkali/alkaline metal salt, BM^+—biopolymer–metal salt complex, X^-—anion part of the salt. In other words, dissociated cations are easily complexed with the aforementioned electron-donating groups, resulting in the rapid ion dissociation process. Hence, ionic transportation occurs via hopping from one coordination site to another site along with polymer segments under the influence of electrical simulation [8,19].

Interestingly, the ion dissociation factor mainly depends on the lattice energy of the doped metal salt. Here, lattice energy is the most important factor for the crystalline compound, depending on the crystal structure and inversely related to the size of the ions. The lower lattice energy results in a higher rate of ion dissociation phenomenon, which leads to increasing the mobile carrier concentration [20]. The ion transfer process primarily occurs via two types of hopping mechanisms, i.e., (i) inter-chain and (ii) intra-chain. The ion-conducting mechanism of the polymer electrolytes is discussed in the following section with a diagram. Various theoretical models were utilized to describe the ion transfer mechanism at elevated temperatures, which contains Arrhenius, Vogel–Tamman–Fulchar (VTF or non-Arrhenius), William–Landel–Ferry (WLF), configurational entropy, and the dynamic percolation model [21–29]. Among various models, Arrhenius and VTF ion conducting mechanisms are treated as dominant types, and the significance of the same is discussed as follows [21]:

1. Arrhenius relationship

The ionic conductivity with respect to temperature obeys the Arrhenius nature (i.e., linear) and the corresponding mathematical expression is:

$$\sigma = A \exp\left(\frac{-E_a}{kT}\right) \tag{2}$$

where A—constant and proportional to the total number of mobile ions, E_a—activation energy, k—Boltzmann constant, and T—temperature in kelvin (K). The Arrhenius relationship demonstrates that the ionic decoupling would create vacancies or voids in the PEs. The nearer mobile ions can occupy voids/vacancies in the polymer chain and re-coordinate with the polymer host. Thus, the ion hopping phenomenon eventually occurs and a greater number of mobile ions are easily detached at the higher temperature [21,22].

2. Vogel–Tamman–Fulchar model

Another significant model used to study ionic transportation in PEs is the VTF model. In this model, temperature-dependent conductivity obeys the non-linear behavior, and the same is expressed as:

$$\sigma = A \exp\left(\frac{-E_a}{T - T_o}\right) \tag{3}$$

where, T_o—temperature corresponding to the zero configurational entropy. As per the nature of the VTF model, non-linear behavior is ascribed to the strong interrelation between the ionic transportation and polymer segments. In other words, segmental relaxation and ionic transportation are coupled with each other [21,23]. More importantly, the free volume of the polymer separators has been increased to the uppermost level at higher temperatures and this is quite commonly noticed behavior in both the Arrhenius/VTF mechanisms. As an output of this, a huge number of mobile charges are coupled/decoupled with the polymer segments, which aids the conductivity and transportation at a greater level.

Despite the fact that the ion-conducting mechanisms of the synthetic and biopolymer polymer electrolytes are not fully understood yet. Furthermore, it is widely recognized that cations are interconnected and re-coordinated with the functional groups of the host polymer [8,21]. Noteworthy, ionic migration mainly occurs in the amorphous regime rather than the crystalline domains. As amorphous nature reduces the energy barrier between the active coordination sites thereby promoting the ionic transportation with polymer segments.

3. Challenges Faced by All Solid-State Electrical Systems

Compared to the liquid electrolyte systems, all solid-state devices exhibit greater safety and compactness; meanwhile, it is trying to reach commercial viability. However, a few serious problems still persist such as lower ionic conductivity and ion transference number, higher interfacial resistance, lack of understanding of the electrode/electrolyte

interface, the profile of the interfacial chemical potential and electrode reactions during transfer of ions between electrode and electrolyte counterparts [8,10]. In commercial devices, electrolyte liquids absorb on the surface of the electrode and ionic transportation occurs in a more rapid manner whereas in solid-state polymer devices, ionic transportation across the interfacial region is not easier and difficulties co-exist including poor diffusivity and conductivity, which is due to the physical contact between electrode/electrolyte and hinders the device performances.

In general, the ionic conductivity of the samples effectively trust the nature of the ion carrier, ion dissociation factor, polymer functional groups, mobility, size of the carrier, crystallinity of electrolytes, etc. Multiple trials have been performed using various types of ion carrier sources with lower lattice energy salt, and incorporation of ionic liquids, plasticizers, and nanofillers in order to fabricate an electrolyte with higher conductivity. Meanwhile, in trying to achieve good physical and chemical interfacial contact between electrode and electrolyte, several novel ion-conducting systems such as pectin, carrageenan, tamarind seed, starch, and cellulose acetate host-based polysaccharides are being involved and their results are recalled in this review. The chosen polysaccharide-based biopolymers, their extraction sources, and their chemical structures have been pictorially portrayed in Figure 2a,b. More importantly, polysaccharide polymers can be easily converted into electrically active materials, due to the presence of electroactive functionalities in the backbone that are available for the greater ion migration process hopefully. In addition, this review article is designed to fully understand the state of the art of polysaccharide compounds and their contribution to several bio-energy storage and conversion devices.
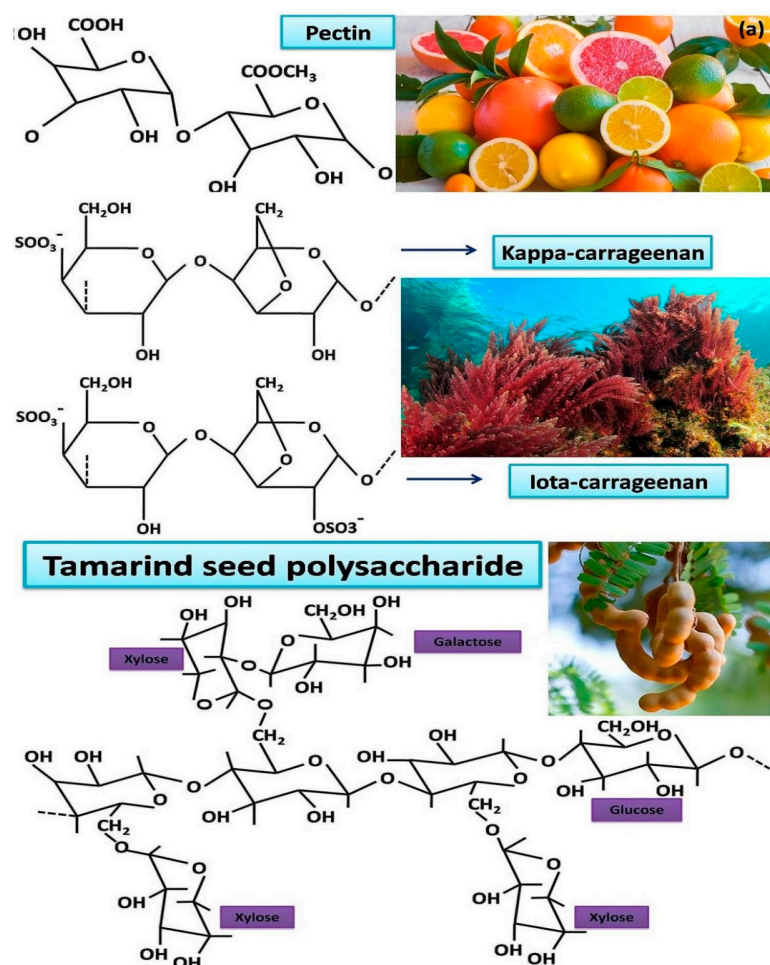

Figure 2. *Cont.*
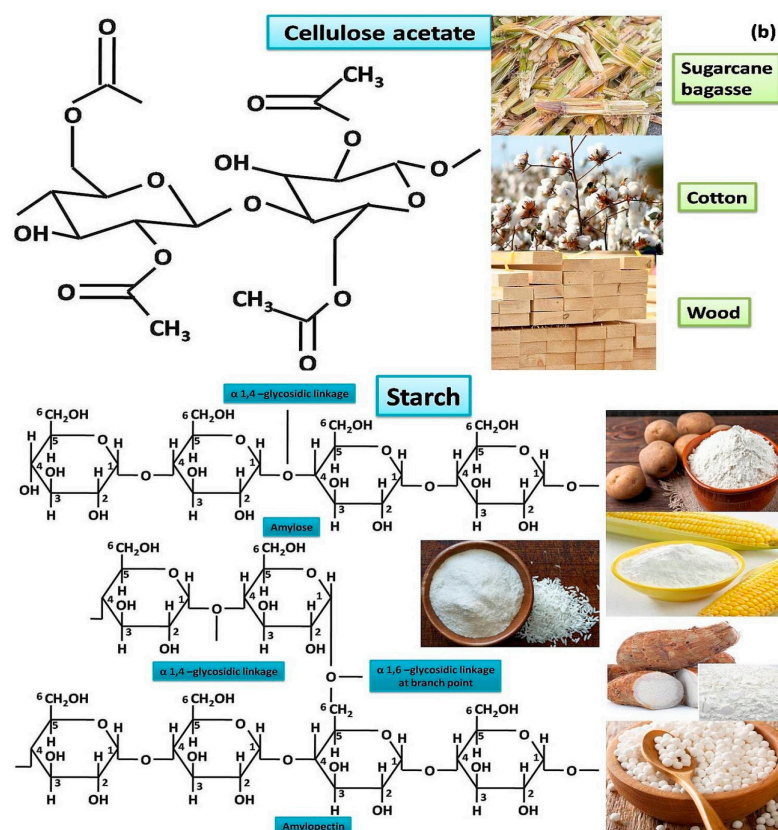
Figure 2. (**a**,**b**) Selected polysaccharide-based bio-matrixes and their extraction sources.

4. Ion-Conducting Biopolymer Systems

4.1. Pectin-Based Biopolymer Electrolytes

Pectin is one of the heterogeneous macromolecules and belongs to a family of complex polysaccharides which is naturally found in the cell wall of plants and derived from citrus fruits skin. The chemical structure of the same contains primarily a polymer of D-galacturonic acid (homopolymer of [1→4] α-D-galactopyranosyluronic acid units with varying degrees of carboxyl groups methylesterified) and rhamnogalacturonan (heteropolymer of repeating [1→2]) α-L-rhamnosyl-[1-L] α-D-galactosyluronic acid disaccharide units), accomplished an α-D-galacturonan. The presence of hydroxyl groups of D-galacturonic acid at the carbon atom 1 and 4 on their axial position, leads to the formation of 1,4-polysaccharide, resulting in the L-1,4-glycosidic linkages between pyranose rings of D-galacturonic acid entities [3,30–32]. In addition, pectin is an anionic polysaccharide and its anionic nature has the higher capability to form a coordination site with doped alkali/alkaline metal cations, which promotes ion dissociation phenomena and enhances the ionic conductivity of the electrolyte system via increasing the concentration of free ions [3].

For example, our research group explored the pectin-based SBEs with the incorporation of several lithium sources and are prepared by trouble-free solution casting route [3,33,34]. At first, the combination of 50 (M.wt%) pectin: 50 (M.wt%) LiCl shows the highest conductivity of 2.08×10^{-3} Scm^{-1}. Increasing the composition of LiCl, diffusion coefficients, and mobility of mobile ion carriers are increased, which supports the larger ionic transportations with polymer segments [33]. On the one hand, the impact of LiCl and LiClO$_4$ on the structural and electrical properties of the pectin membrane has been inspected and reported independently [34]. The lower charge transfer resistance is noticed for the cell consisting of Zn-metal powder, 50 (M.wt%) pectin: 50 (M.wt%) LiCl and LiFePO$_4$ used as an anode, electrolyte, and cathode respectively. The result indicates that the as-prepared pectin electrolyte holds good compatibility among Zn and LiFePO$_4$ electrodes and positively guides toward the design and fabrication of pectin-based Li-ion

migrating electrolytes in the next biopolymer battery chemistry. Another survey reveals the effect of ethylene carbonate (EC-plasticizer) on the physicochemical and electrochemical properties of pectin with the $LiClO_4$ complex, explored by Perumal et al. [3]. The pectin with $LiClO_4$ complex records the conductivity of 5.15×10^{-5} Scm^{-1}. The noticed conductivity value is lesser when compared to LiCl incorporated pectin system but lattice energy is low for the $LiClO_4$ salt rather than LiCl. The low lattice energy provides easier solvation of cations thereby being able to coordinate with the oxygen constituents of the macromolecular backbone. In contrast, higher conductivity is noticed for the LiCl: pectin sample, which is due to the utmost amorphous behavior and more creation of free volume within the molecular regimes. The conductivity of the electrolyte is strongly based on the nature of the ion species, concentration, lattice energy of the selected salt, amorphous portion and free volume, diffusivity and mobility of the cations. As a consequence, pectin: LiCl shows a higher Li$^+$ conductivity rather than the low lattice energy salt ($LiClO_4$) added pectin sample.

In order to increase the Li-ion conductivity, various concentrations of EC are added to the pectin: $LiClO_4$ complex and results in crystallinity reduction via structural modifications that ensure frequent structural interruptions. In the case of BEs, the ionic conduction process mainly occurs in the amorphous phase rather than crystalline regions. The amorphous phase improves ionic transportation through its flexible character with inter- and intra-chain motion which aids to acquire higher ionic conductivity and the value is 3.89×10^{-4} Scm^{-1}. Plasticizer has a higher dielectric constant and is able to dissociate a greater number of Li-ions, thus proves that the absence of ion pair formation. As a result, an increment in the production of charge carriers leads to obtaining higher ionic conductivity. Similarly, Andrate et al. [32] also studied the effect of glycerol on the pectin: $LiClO_4$ complex and this study shows the plasticized pectin electrolyte demonstrates the greater Li$^+$ conductivity of 4.7×10^{-4} Scm^{-1}.

It is worth noting that, electrochemical window stability is another mandatory criterion for electrolytes. As ionic conductivity and potential window stability of the electrolytes play a significant role in the electrical performance of the device. Interestingly, the window of electrochemical stability is improved from 3.39 V (un-plasticized sample) to 3.55 V for the pectin: $LiClO_4$-EC plasticizer added sample. The primary battery study resembles that the obtained open circuit potential (OCP) is used to light up the LEDs. Thus, further evidence that the practical utility of the prepared BEs towards battery operations [3]. However, the incorporation of plasticizer as an additive leads to reducing the mechanical strength and stability of the PEs. This drawback could be overwhelmed by the introduction of metal oxide particles in PEs as a filler and comes under the composite polymer electrolytes category. The incorporation of nanoparticles into the host, ionic conductivity of the same has been improved via percolating interfacial effect and providing excellent mechanical strength to the polymer electrolytes.

Pectin cross-linked with glutaraldehyde results in the amidated pectin membrane, reported by Mishra et al. [35]. The amidation process influences the chemical properties of the pectin host in terms of altering their functional groups and molecular interactions. This amidated pectin is replaced with the low methoxy pectin and attains its ionic conduction capability. The degree of the amidation process has been supported by the results of elemental and FTIR analysis. The covalent bond formation between the pectin chain and amide is evidenced by the monitored vibrational bands at 1672 and 1595 cm^{-1}, which are attributed to amide I and amide II, respectively. After the amidation process, the percentage of water uptake seems to be greatly improved and helps to achieve the highest proton conductivity of 1.09×10^{-3} Scm^{-1}. Another survey discusses the impact of NH_4SCN on the pectin macromolecular electrolytes, investigated by Muthukrishnan et al. [36]. Increment in the concentration of the NH_4SCN source, the relative intensity of the vibrational bands has been tuned and reveals the production of a higher number of free H-ions. Thus, enriches the proton conductivity to the uppermost level of 1.5×10^{-3} Scm^{-1}. This result is well agreed with the transference number analysis and the maximum number of 0.96 is noticed

for the composition of 40 pectin: 60 NH_4SCN. The assembled primary proton device shows a stabilized OCP of 1.45 V and it is suitable for low-current-density applications [36].

More importantly, the research attempts on novel ion-conducting electrolytes are highly commendable and able to deliver better electrochemical performance when compared to existing electrolyte systems. Other than Li-battery technology, Na^+, Mg^{2+}, Mg/air, and Zn^{2+} batteries are upcoming filed of energy research and science technology. In this concern, magnesium ion batteries (MIBs) are an excellent alternative and are considered a cost-effective one. Furthermore, Mg is an earth-abundant, inexpensive, eco-friendly, and easy-handling material when compared to lithium. For instance, Kiruthika et al. [37,38] studied the pectin-based Mg-ion conducting electrolytes and $Mg(NO_3)_2$ has been used as a Mg-ion provider source. They have reported the maximum Mg-ion conductivity of 7.7×10^{-4} Scm^{-1} for the composition of 50 pectin: 50 $Mg(NO_3)_2$. Using this membrane, the Mg-battery has been fabricated and exhibited an OCP of 1.82 V at room temperature.

Based on the above finding and results, Mg-ion conducting electrolytes are cost-effective novel materials for the next century energy storage devices. Moreover, the same author has explored the effect of $MgCl_2$ on the various properties of pectin electrolytes. This finding indicates that the composition of 30 (M.wt%) pectin: 70 (M.wt%) $MgCl_2$ shows the highest Mg-conductivity of 1.14×10^{-3} Scm^{-1} with the transference number of 0.30 and exhibits the window stability of 2.05 V. The primary device was conducted using Mg-metal, MnO_2/graphite, and above highest complex as an anode, cathode, and electrolyte, respectively, and demonstrates the OCP of 2.16 V. The various alkali metal salt incorporated pectin-based electrolytes [39–43] and their ionic conductivity values are bar graphically represented in Figure 3. Based on the discussion, most of the pectin-based ion conducting system exhibits the ionic conductivity range from 10^{-3} to 10^{-4} Scm^{-1}. Interestingly, plasticized pectin with $LiClO_4$ shows the highest window stability of 3.55 V compared to other pectin samples, which is suitable material for the device analysis [3].
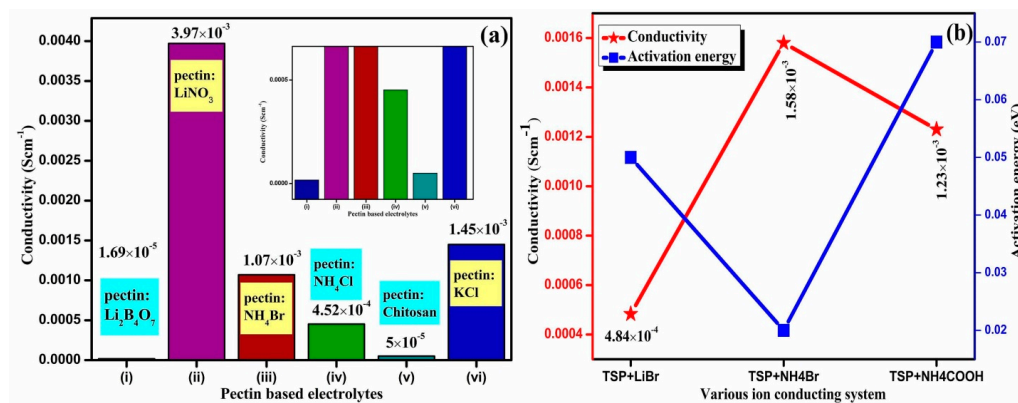

Figure 3. (**a**) Bar notation of pectin-based electrolytes with addition of various metal salts, (**b**) several electrochemical properties of H^+ and Li^+ conducting TSP-based electrolytes.

4.2. Carrageenan-Based Ion-Conducting Electrolytes

Carrageenan is an anionic carbohydrate polymer and is derived from the chancrous crispus spies of seaweed [44]. The chemical structure of carrageenan consists of alternating 1,3-linked α-D-galactopyranose and 1,4 linked β-(3,6-anhydro) D-galactopyranose. Moreover, it can be broadly classified into three types, which are kappa carrageenan (k-carrageenan-$C_{24}H_{36}O_{25}S_2{}^{-2}$), iota-carrageenan (i-carrageeenan-$C_{24}H_{34}O_{31}S_4{}^{-4}$), and lambda carrageenan (λ-carrageenan-$C_{12}H_{19}O_{20}S_3{}^{-3}$) [45]. The main dissimilarity exists in the negative disaccharide units, sulfate, and electron-donating groups among the varieties of carrageenan. It can be extensively used in the food industries as a stabilizer, thickener, emulsifier, and gelling agent and is also used in the pharmaceutical as well as cosmetic industries [46].

In 2020, Zainuddin and co-workers [47] deals with the characterization of blend hybrid electrolytes, and the same is composed of 80 carboxyl methyl cellulose and 20 kappa-

carrageenan (K-C). Various concentration of NH_4NO_3 is included as a proton source in the hybrid matrix and their physical & chemical changes have been studied with the help of several analytical techniques. As a matter of fact, free ion percentage plays an important role in the protonation process of prepared hybrid membranes. As added proton salt has been dissociated into NH_4^+ and NO_3^-, in which proton ions come from NH_4^+ and can be able to connect with the oxygen atoms of hybrid chains thereby producing more free ions. Thus, decreases the energy barrier of polymer segments and results in a higher number of protonic transportations via inter- and intra-chain hopping processes. The obtained value of maximum free ion percentage is 63.25% for an 80:20 blended host with the addition of 30 wt% proton source (NH_4NO_3). This result is well reflected in the proton conductivity analysis and demonstrates the highest H-conductivity of 2×10^{-4} Scm^{-1}. Furthermore, K-C with NH_4SCN complex shows the proton conductivity of 6.8×10^{-4} Scm^{-1}, reported by Christopher Selvin et al. [48]. Noteworthy, NH_4SCN salt has lesser lattice dissociation energy than that of NH_4NO_3 hence the generation of more amount of free H^+ and further leads to achieving excellent H-conductivity. On the other hand, iota-carrageenan (i-c) with $LiNO_3$ displays the Li-ion conductivity of 5.85×10^{-3} Scm^{-1} [49]. Carrageenan-based various ion conducting samples and their electrical values are summarized in Table 1 [49–59].

Table 1. Carrageenan-based various ion conducting electrolytes and their electrochemical performances.

| Electrolyte Composition	Conductivity (10^{-3}) (Scm^{-1})	Window Stability (V)	Activation Energy (eV)	References
K-C+$LiNO_3$	5.51	3.1	-	Mobarak et al. [49]
K-C+LiBr	3.43	3.5	0.08	Arockia Mary et al. [50]
K-C+NH_4Br	0.38	-	-	Zainuddin et al. [51]
i-C+LiCl	5.33	-	0.19	Chitra et al. [52]
i-C+$LiClO_4$ i-C+$LiClO_4$+SN	0.35 3.33	2.36 3.10	0.22 0.10	Chitra et al. [53]
i-C+NH_4Br	1.08	2.1	0.18	Karthikeyan et al. [54]
i-C+NH_4NO_3	1.43	2.46	0.14	Moniha et al. [55]
i-C+NH_4SCN	3.56	3.19	0.21	Moniha et al. [56]
i-C+$Mg(NO_3)_2$	0.61	-	0.175	Shanmugapriya et al. [57]
i-C+$Mg(ClO_4)_2$	2.18	-	0.055	Shanmugapriya et al. [58]
Carboxymethyl Carrageenan (CMC)+BmImCl	5.76	3	-	Shamsudin et al. [17]
CMC+NH_4I+ Glycerol	3.9	-	-	Torres et al. [59]

4.3. Tamarind Seed Polysaccharide-Based Electrolyte Membranes

Tamarind seed polysaccharide (TSP) is a highly branched carbohydrate polymer obtained from the seed of Tamarind indicia L [60]. The chemical arrangement of TSP contains β-(1,4)-D-glucan substituted with the side chains of α (1,4)-D-xylopyranse and (1,6) linked {β-D-galactopyranoseyl-(1,2)-α-D-xylopyranosyl} to residues of the glucose. Glucose, xylose, and galactose are present in the monomer with ratios of 2.8:2.25:1.0 [61]. TSP is insoluble in organic solvents and cold water as well. However, TSP has some unique characteristics such as non-ionic, neutral, tasteless, high thermal and chemical stability, forming viscous gel solution with a broad range of pH tolerance, non-carcinogenicity, mucoadhesivity, and adhesivity [62,63]. From the perspective of electrochemical devices, the TSP macromolecule demonstrates better energy storage performance and is extremely rich in electron-donating groups on their backbone, hence molecular coordination/interaction would occur in a rapid manner. For instance, Li-ion conducting TSP membrane shows the

highest conductivity of 6.7×10^{-3} Scm^{-1} among other TSP-based samples which is ascribed to the low value of T_g and crystallinity percentage. The incorporation of LiCl salt leads to enriching the flexibility of TSP polymer segments in turn to acquire utmost conductivity. These results are perfectly indexed with the dielectric, mobility, and transference number analysis [64]. In the same vein, NH$_4$SCN incorporated TSP shows the H-conductivity value of 2.85×10^{-4} Scm^{-1} which is due to an increment in the concentration of proton carriers. In the H-ion system, H-ion transportation occurs from the loosely bounded H$^+$ in the dissociated NH$_4^+$ cation part via vehicular or Grotthuss-type mechanisms [61]. The noticed H-conductivity value is lower when compared to the Li-conducting TSP sample [64] and this might be due to changes in the nature of the source cation and molecular orientation between TSP polymer as well as incorporated additives.

The majorly accepted H-ion transport mechanisms are Grotthuss (hopping) and vehicular (diffusion). In the hopping process, H-ion jumps from one site to another site with varying potential energy as well as energy barrier of the same. Furthermore, H-ion motion mainly depends on the formation rate and bonding formation among hydronium ions as well as water molecules. To sum up, H-ions migrate from one co-ordinate spot to another spot via a hopping process with lesser activation energy. Whereas vehicular mechanism involves the complex formation of proton and water molecule then diffuse/penetrates through the polymer backbone. Another main difference between the hopping and diffusion mechanism is the formation of a hydrogen bond. During the hopping mechanism, a strong hydrogen bond is formed whereas a weaker H-bond is formed in the case of diffusion or vehicular mechanism [2,65–67]. On the other hand, proposed Li$^+$ conducting mechanisms take place via inter-chain hopping (segmental motion) or intra-chain (ion-dipole) process. Incorporated additives or Li-salts into the host matrix, the dissociated Li-ions is interacted or form a transient covalent bond with the oxygen atoms or electron-donating groups in the biopolymer backbone. For the interchain process, the complexed Li-ion is hopping from one polar site to another polar site along with segmental motion and marked as a red arrow in the Scheme 1. In the case of intra-chain or jumping, dissociated Li-ions jump from one transient site to another vacant site with an ionic decoupling process and are indicated as a dotted line in Scheme 1 [49,68,69].

Recently, Sampath et al. [70] have investigated the impact of plasticizers on the TSP-based Li-ion conducting electrolytes. The plasticizer-added sample displays the maximum Li-ion conductivity of 1.06×10^{-3} Scm^{-1} which is one order of magnitude larger than the un-plasticized composition. This finding substantiates that the impregnation of the plasticizer helps to increase the conductivity via promoting the amorphous region as well as free volume of the electrolytes and also leads to enriching the electrochemical stability window of the TSP sample to the maximum value of 2.98 V. In addition to that, TSP-based Mg-ion conducting electrolytes were also studied and reported by our research team [71]. TSP with Mg(ClO$_4$)$_2$ complex records the maximum conductivity of 5.66×10^{-4} Scm^{-1}. Thermal stability and electrochemical stability properties are found to be increased while increasing the content of Mg(ClO$_4$)$_2$. The maximum Mg-ion conducting sample shows the window stability of 3.93 V whereas pure TSP film can be stable up to 2.85 V. Temperature-dependent analysis reveals that the involvement of Arrhenius type of ion conducting mechanism in the current system and shows the lowest E_a value (0.09 eV). The primary Mg-battery has been fabricated by enabling MnO$_2$ and mixed proportion of V$_2$O$_5$ and PbO$_2$ as a cathode material and shows the OCP values of 2.12 and 2.36 V, respectively. Furthermore, with the addition of salt, the wettable nature of the sample is dropped when compared to salt-free film, as observed from the results of the contact angle study. Noteworthy ionic, thermal, transference number, and window stability properties are increased with the addition of Mg(ClO$_4$)$_2$. This may be due to the incorporation of salt changes in the host polymer properties via interaction, interruptions, and complexation phenomena. Various tamarind-seed-assisted Li-ion and H-ion conducting electrolyte membrane [72–74] results are pictorially given in Figure 3b.
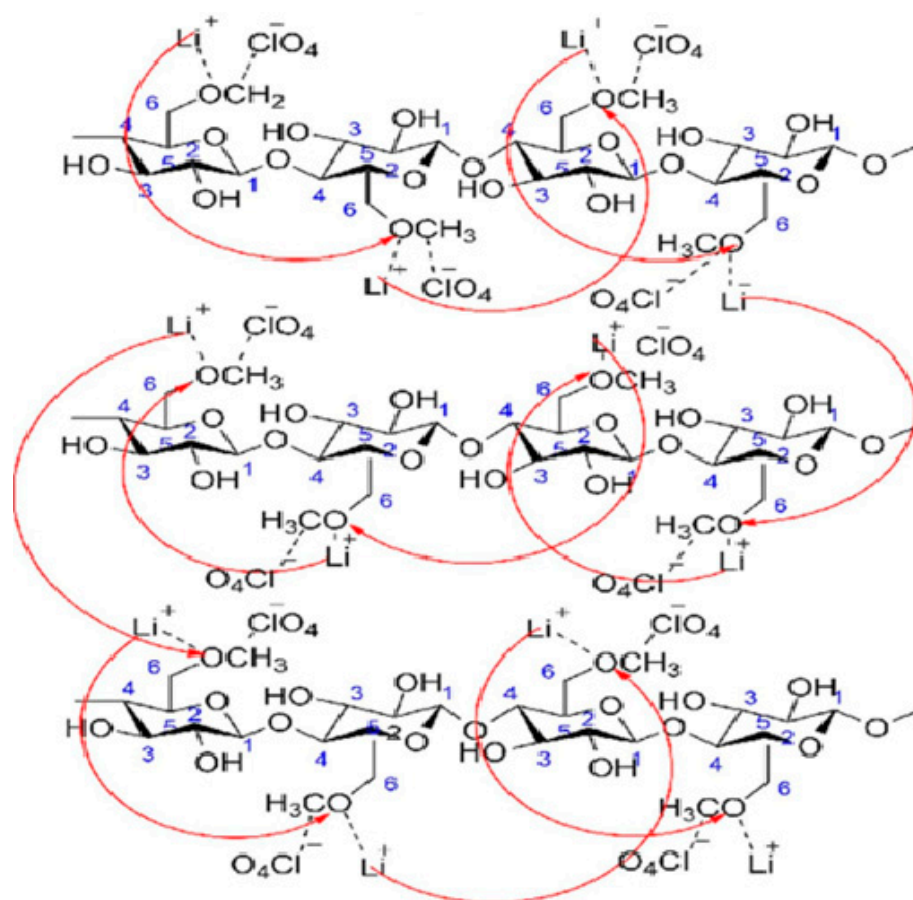
Scheme 1. Proposed mechanism of MC-LiClO$_4$ complex and hopping Li$^+$ ions: the curved red (arrow) arrows depict the possibility of Li$^+$ ions hopping through the MC backbone, while the broken lines (- - - -) represent ion–dipole interactions between the Li$^+$ ions as well as ClO$_4^-$ ions and the polar functional groups of the MC structure with permission [68].

4.4. Cellulose Acetate-Based Electrolytes

Cellulose is a familiar bio-product and its chemical structure is nearly close to that of starch products with a slight difference in their glycosidic rings i.e., β-1,4 glycosidic rings. Among different kinds of cellulose derivatives, cellulose acetate (CA) natural product has received remarkable attention due to their superior properties including earth abundance, good transparency, and chemical stability [75]. The main hindering factor of CA is its high crystalline nature and higher value of T$_g$ [75,76]. Hence, in order to find solutions against the issues of CA, blending of the host, plasticizer, metal salts, filler, and ionic liquids is generally preferred thereby able to hold their functionalization in energy devices.

For example, Ramesh et al. [75] attempted to prepare CA-based polymer gel membranes with the addition of both metal salt (LiTFSI) and ionic liquid (AmImCl), resulting in the highest Li$^+$ conductivity of 1.07×10^{-3} Scm^{-1}. The reason for conductivity improvement is ascribed to the detachment of bonding within the atoms of oxygen and acetate group, which is evidenced by the shifting of C=O stretching vibration. Thus, provides more availability of empty oxygen to aid the mobility of Li-cations, which assists the hopping process from one free site to another site. The impact of various proton sources in CA hosts is studied by Monisha et al. [77,78]. They have found that the maximized proton conductivity of 3.31×10^{-3} and 1.02×10^{-3} Scm^{-1} for NH$_4$SCN and NH$_4$NO$_3$ complex respectively.

Another survey on CA with LiNO$_3$ and LiClO$_4$ shows the conductivity values of 1.93×10^{-3} Scm^{-1} and 1.79×10^{-4} Scm^{-1}. In addition, LiNO$_3$-added samples demonstrate the utmost window stability of 4.09 V [79,80]. Leonarda and co-workers [81] have

synthesized edible cellulose-based composite electrolytes for supercapacitors. As-prepared composite conductive films exhibit a low resistivity of 10 Ω cm. the mechanical and electrical performance of the prepared films has been tuned via the incorporation of several additives such as myristic acid, citric acid, and sunflower oil. The combo of ethyl cellulose and activated carbon serves as a good candidate for green electronics applications. Important to note that, several review themes corresponding to cellulose-based derivatives are hugely available and reported recently [82,83].

4.5. Starch and Their Derivatives-Based Ion Conducting Electrolytes

Starch is an incredibly important natural product among biomass groups and strongly depends on their extraction sources. More specifically to mention that starch matrix has been widely classified into different types, which are named potato starch, corn starch, sago starch, rice starch, arrowroot starch, etc. In this section, the authors are clearing up in detail the above-mentioned starch-related BEs towards the various electrochemical aspects. Starch plays a major role to store plant tissues and its chemical structure is composed of linear amylose (poly-α1,4-D-galacopyronoside) and extremely branched amylopectin (poly-α1,4-D-galacopyronoside and poly-α1,6-D-galacopyronoside)groups [84].

A linear amylose group contains 200 to 20,000 glucose units on its background, thus leading to it to form a helix structure. Whereas amylopectin has 30 side chains of glucose and are connected to the head of the chain with all the 30 glucose units thereby forming a branched chain. Starch has good properties of solubility and adhesion nature but its mechanical stability is low when compared to other polysaccharides which are due to their hydrophilic nature [85,86]. Hence, various strategies have been followed to enrich the mechanical properties and ionic conducting capacities to be held as the electrolytes for emerging electrochemical applications.

Hamsan et al. [87] have performed potato starch and methyl-cellulose-based plasticized blend electrolytes with the incorporation of NH_4NO_3 towards the EDLC operation. With the incorporation of glycerol, ionic conductivity of the current blend electrolytes is improved at the same time followed by the non-Arrhenius type of ionic transportations. In VTF behavior, proton conductivity is dominated by the movements of ions with polymer segments via free volume. The maximum conductivity of the order of 10^{-3} Scm^{-1} and window stability of 1.88 V is achieved for the 40 wt% glycerol added blended host with salt complex.

Khanmairzaei et al. [88] have reported the effect of 1-methyl-3-propylimidazolium iodide (ionic liquid) on various functional properties of Na^+ conducting rice starch electrolytes. They have obtained the highest Na-ion conductivity value of 1.20×10^{-3} Scm^{-1} which is supported by the amorphous nature of the same. Notably, electrical parameters of the starch-based electrolytes with the incorporation of several metal salt, plasticizer, and ionic liquids are summarized in Table 2 (Refs. [89–125]).

In all of the discussed biopolymer ionic systems, salt concentration plays a significant role and heavily stimulus the conductivity properties. The optimum salt concentration, plasticizer, and filler incorporated biopolymer system exhibit the maximized ion conducting property including Li^+, Mg^{2+}, H^+, and Na^+. This is due to the threshold holding of added additives in the backbone of the polymer network. After the optimum concentration, the polymer network does not have the capacity to accommodate external additives and leads to the ionic clusters/pair formation thus affecting the mobility of charge carriers thereby reducing the ionic conductivity values. Importantly, biomass-based products have been placed in a good position in scientific research and soon they will be reaching commercial viability for the upcoming eco-friendly and clean electrical gadgets.

Table 2. Electrochemical performance of the starch-based membranes.

Electrolyte Composition	Conductivity (Scm^{-1})	Activation Energy (eV)	References
Solid polymer electrolytes			
PS-GA-NaI	3.41×10^{-2}	-	Madhavi Yadav [89]
PS-GA-NaI PS-GA-NaSCN PS-GA-NaClO$_4$	7.19×10^{-6} 1.22×10^{-5} 1.12×10^{-4}	-	Tuhina Tiwari, [90]
RS-LiI	4.68×10^{-5}	0.41	Khanmirzaei [91]
PS-Methylcellulose (MC)-NH$_4$NO$_3$	4.37×10^{-5}	0.30	Hamsan [92]
PS-LiI PS-NH$_4$I PS-NaI	4.68×10^{-5} 1.39×10^{-4} 4.79×10^{-4}	0.41 0.16 0.11	Khanmirzaei [93]
Starch-NH$_4$NO$_3$	2.83×10^{-5}	0.41	Ahmad Khiar Khair [94]
CS-LiClO$_4$	1.55×10^{-6}	0.64	Teoh [95]
AS-NaI-GA	6.7×10^{-4}	-	Tiwari [96]
PS-PEG-NaI-GA	1.8×10^{-4}	-	Tiwari [97]
RS-NaClO$_4$-GA	1.59×10^{-2}	-	Yadav [98]
RS-LiI-I$_2$	-	-	Yoganda [99]
CS-Chitosan-NaI	3.04×10^{-4}	0.2	Yusof [100]
Starch-KI	3.46×10^{-3}	-	Bementa [101]
PVA-Starch-GA-NH$_4$SCN	1.31×10^{-4}	-	Kulshresthagupta [102]
Composite electrolytes			
CS-LiClO$_4$-SiO$_2$	1.23×10^{-4}	0.25	Teoh [103]
CS-LiClO$_4$-BaTiO$_3$	1.84×10^{-4}	-	Teoh [104]
Plasticized/ionic liquid added systems			
PS-Chitosan-LiCF$_3$SO$_3$-Glycerol	1.32×10^{-3}	0.11	Amran [105]
CS-LiClO$_4$-Glycerol	1.1×10^{-4}	-	Marcondas [106]
SS-glycerol (LiClO$_4$) NaCl NaClO$_4$ Na$_2$SO$_4$ LiCl KCl	9.91×10^{-4} 2.55×10^{-3} 1.38×10^{-3} 5.23×10^{-4} 3.37×10^{-3} 3.80×10^{-3}	0.39 0.21 0.26 0.38 0.23 0.11	Pang [107]
CS-LiI-Glycerol	9.56×10^{-4}	0.16	Shukur [108]
CS-LiClO$_4$-Glycerol	1.2×10^{-3}	-	B. Aziz [109]
CS-Chitosan-NH$_4$Cl-Glycerol	5.11×10^{-4}	0.19	Shukur [110,111]
CS-NH$_4$Br-Glycerol	1.8×10^{-3}	0.11	Shukur [112]
CS-Chitosan-NaI-Glycerol	1.28×10^{-3}	0.18	Yusof [113]
PS-MC-NH$_4$NO$_3$-Glycerol	-	-	Hamsan [114]
PS-MC-LiClO$_4$-Glycerol	4.25×10^{-4}	0.165	Yusof [115]
CS-Chitosan-NH$_4$I-Glycerol	-	-	Yusof [116]

Table 2. *Cont.*

Electrolyte Composition	Conductivity (Scm^{-1})	Activation Energy (eV)	References
CS-Chitosan-NH$_4$Br-EC	1.44×10^{-3}	0.17	Shukur [117,118]
RS-LiI-1-methyl-3-propylimidazolium iodide-TiO$_2$	3.63×10^{-4}	0.22	Khan [119]
CS-LiPF$_6$-BmImPF$_6$	1.47×10^{-4}	0.0085	Liew [120]
CS-LiPF$_6$-BmImTf	3.21×10^{-4}	-	Liew [121]
CS-LiPF$_6$	1.03×10^{-3}	-	Ramesh [122]
PS-Mg(C$_2$H$_3$O$_2$)$_2$-Glycerol-BmImCl	1.12×10^{-5}	-	Shukur [123]
PS-GO-LiCF$_3$SO$_3$-BmImCl	4.80×10^{-4}	-	Azli [124]
CS-LiTFSI-AmImCl	4.18×10^{-4}	-	Ramesh [125]

5. Recent Progress in the Biopolymer-Inspired Electrochemical Devices

Nowadays, pioneering work on the BEs and their application in several kinds of electrical devices are summarized briefly in this section in order to provide new insights in the direction of developing the safety-reinforced and advanced greener energy applications.

5.1. Solid-State Polymer Batteries

LIBs are widely recognized in numerous portable electrical devices and significantly impact the world energy market as a potential power system among other battery chemistries. Unfortunately, it would have some drawbacks such as poor electrochemical performance, safety, environmental standards, and higher cost. Hence, a battery with rich electrochemical properties, a longer life span, and safety parameters has been considered as a core power technology for higher energy applications. So, the development of new battery chemistry is an excellent alternative to the use of the above-discussed biopolymer electrolytes. Herein, the authors are discussing the electrochemical operations of several types of batteries, which includes Zn-ion, metal–air, and solid-state polymer batteries.

Research on these battery technologies is crucial for the successful implementation of the emerging electrical market and wearable products [126]. Rechargeable battery performance of the pectin and tamarind seed polysaccharide-based ion conducting electrolytes has not been implemented which is in the preliminary level of understanding. Meanwhile, it can be employed in primary battery studies and their results are discussed in the respective introductory part of the ion-conducting systems. On the other hand, a flexible quasi-Zn-ion solid-state battery has been tested using the highest ion-conducting carrageenan electrolytes, explored by Yuan Huang et al. [126]. The fabricated quasi solid-state battery delivers an excellent electrochemical performance and rate capacity as well as cycling stability. This may be due to the utmost higher ionic conductivity of the electrolyte and enhancement in the charge transport mechanism across the interfacial region of the assembled device. Thus, a maximum specific capacity of 291.5 mAhg^{-1} at the current rate of 0.15 Ag^{-1} is attained.

Leng et al. [127], studied the gel composite electrolytes based on a blended polymer host, which consists of CA and PVdF-HFP for Li-O$_2$ battery. The Li-air battery has delivered an excellent energy density of 11,140 Whkg^{-1} which means that it is 10 times greater than the energy density of present LIBs. The coin cell has been assembled using air, Li-foil, and CA/PVdF-HFP as cathode, anode, and electrolyte, respectively. In this work, the authors have explored the comparison battery performance of as-prepared polymer gel electrolytes and liquid electrolytes (LE). The prepared GPE is stable up to 4.7 V vs. Li and shows a conductivity of 5.49×10^{-4} Scm^{-1}. However, LE assisted battery exhibits a larger discharge capacity than that of GPE used battery and their discharge curve is compared in

Figure 4i(a,b). At the same time, GPE employed battery displays superior cycling stability which is proved by the EIS analysis. During the cycling process, the value of R_{ct} seems to be low which is evidence that the GPE displays a good cycling nature and possibly prevents the Li_2O_2 attack. The insight mechanism of the interfacial effect has been studied by post-assembly of the cell and their photographs are presented in Figure 4ii. After 20 cycles, a thick black film is observed for the LE-enabled battery whereas GPE used battery shows the slightly black layer and represented in Figure 4ii(a–f). The noticed superior stability of the GPE battery may be due to prohibiting the impact of oxygen diffusion and LiOH passivating film on the Li-anode. From these findings, as-prepared GPE is an excellent prime candidate for the LIBs and metal–air batteries.
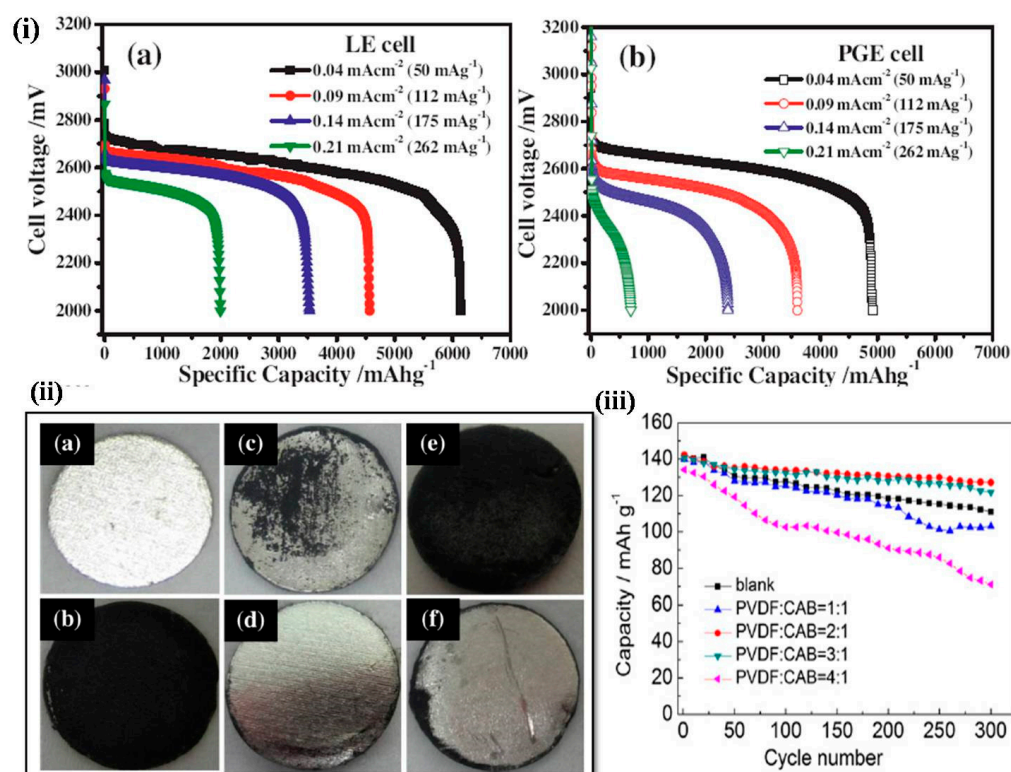

Figure 4. (**i**) Li-air battery performance of using (**a**) liquid electrolyte, (**b**) gel polymer electrolyte. (**ii**) Photographs of Li anode: (**a**) pristine; (**b**) after exposure to air atmosphere; (**c**) disassembled from the PGE battery after 20 test cycles, the side contacting on PGE membrane, and (**d**) the side contacting current collector; (**e**) disassembled from the liquid electrolyte battery after 20 test cycles, the side contacting on the PE separator, and (**f**) the side contacting on current collector (reproduced from Ref. [127] with permission). (**iii**) Cycle performances of $LiCoO_2$/PE-liquid electrolyte/ graphite and $LiCoO_2$/PE supported GPEs with different ratios of PVDF to CAB/graphite batteries, charged and discharged with 1C rate at room temperature (Reproduced from Ref. [128] with permission).

Moreover, the effect of PE on the blend composition of CA butyrate (CAB)-PVdF is elucidated by Liu et al. [128]. The CA butyrate (CAB)-PVdF with PE-supported blend composition displays good compatibility between electrode/electrolyte and shows the maximum stability window of 4.7 V which is more dominant than that of gel electrolyte without PE addition. Battery performance of graphite/PVDF: CAB-PE-supported GPE/$LiCoO_2$ shows a higher discharge capacity with greater capacity retention of 93.1% after 300 cycles (Figure 4iii). This enhanced performance of the battery may be attributed to the highest ionic conductivity of electrolyte (2.48×10^{-3} Scm^{-1}) and wonderful interfacial contact. On the other hand, cellulose triacetate-poly(polyethylene glycol methacrylate) based gel membrane employed battery shows the superior discharge capacity of 164 $mAhg^{-1}$, which

is due to a higher value of transference number (0.7) and conductivity, investigated by Nirmale [129].

Notably, the impact of SiO_2 nanoparticles on the PVdF-CAB-PE supported blended gel polymer electrolytes is studied by Zhao et al. [130]. From the effect of SiO_2, the thermal stability of the electrolyte is greatly improved. As a result of this, the contact between anode and cathode is disallowed thereby enhancing the safety of the device. Furthermore, improves the decomposition potential of the electrolyte, and the value is found to be 5.2 V. Incorporation of SiO_2 results in greater compatibility between electrode and electrolyte interface and displays a good discharge capacity of 145 mAhg^{-1} with the capacity retention of 94% when compared to without SiO_2 assisted device.

More importantly, Lin et al. [131], explored the starch-based membranes for the application of all-solid-state lithium–sulfur batteries for the first time. Corn starch with LiTFSI shows the highest Li-ion conductivity of 3.39×10^{-4} Scm^{-1} as result higher transference number of (0.80) is inferred from the chronoamperometry study. The highly conducting starch electrolyte is steady up to 4.8 V and the same is higher than the window stability of a commercial liquid system (4.2 V). The coin cell has been constructed with the geometry of Li/starch+LiTFSI/sulfur. The assembled coin cell shows the maximum and initial specific capacity of 1442 mAhg^{-1} at 1C rate and after the multiple cycles, the initial capacity of the same is reduced to the value of 864 mAhg^{-1}. Based on these results, we can substantiate the use of biomaterials as an electrolyte compound for the forthcoming eco-friendly solid-state electrical gadgets.

5.2. Supercapacitors

Supercapacitors or ultra-capacitors are the most influential energy devices and are believed to be promising energy devices in the future which demonstrates the higher power density, stable lifespan, and fast recharging capability. Depending on the chemistry and electrochemical behavior of the materials, they can be divided into EDLC, pseudo, hybrid, and Li-ion hybrid capacitors. Among myriad classifications, EDLC received wider attention due to its technical merits. The charge storage mechanism of EDLC relies on electro statistical accumulation of charges on the electrode/electrolyte boundary with high surface area carbon-based electrodes [132]. Despite that, the energy density of electrochemical capacitors is not sufficient for higher energy operations. Therefore, multiple trials have been devoted to fabricating new electrolytes with a wider potential window.

Recently, carrageenan-based hybrid electrolytes enabled EDLC has been fabricated with the use of activated carbon electrodes, reported by Zainuddin and co-workers [47]. The shape of the noticed CV pattern does not contain any oxidation and reduction peaks thereby confirming the formation of the electric double layer. Furthermore, there is not much difference in the shape of the rectangular pattern while increasing the sweep rates at the same time the capacitance of the device gets dropped. The highest specific capacitance of assembled EDLC shows the value of 25.65 Fg^{-1} at 2 mVs^{-1}. This low scan rate provides a greater interfacial compatibility and facilities the proton migrations across the electrode/electrolyte interface and their scheme is illustrated in Figure 5a. Furthermore, the assembled device has been tested by a GCD study and cycled up to 10,000 cycles at 0.2 mAcm^{-2}. After the 10,000 cycles, the stabilized average capacitance of 20 Fg^{-1} is noticed with higher columbic efficiency, and their cycling strength is given in Figure 5b.

It is worth noting that, mechanically stable alkaline gel polymer electrolyte membranes have been studied for supercapacitor operation by Hu et al. [133]. In this work, KOH has been utilized as a dual role carrier, i.e., it can act as an ion provider source as well as a cross-linking agent in the electrolyte samples. Increasing the content of k-carrageenan, ionic conductivity, and water uptake properties are increased rapidly due to a reduction in the crystallinity of the samples as well as the absorption of more water molecules in the alkaline gel membrane. The present results are in good accordance with the porous morphology texture and are confirmed by the FESEM analysis. Supercapacitor has been assembled by employing alkaline gel and PVA-KOH-based electrolytes. From the CV

measurements, the k-carrageenan gel electrolyte-based supercapacitor shows a higher capacitance value (470 Fg^{-1}) than that of the PVA-KOH membrane-assisted device. Moreover, both the electrolyte-assisted device demonstrates the electric double-layer nature, and the same is further tested by GCD analysis with various current densities. From the GCD analysis, a small value of iR drop is noticed for the fabricated EDLC which indicates that the formation of a good electrode/electrolyte interface and assembled device possessed good rate capability (Figure 5c). In order to examine the cycling stability, the fabricated device was cycled to 2000 cycles. After the multiple cycles, fabricated EDLC withhold their capacitance of 95% which proves the stability of the device towards the purpose of practical implementation. Interestingly, pectin and TSP polymer have been further utilized in the preparation of porous carbon electrode material for the application of electrochemical capacitors. Very recently, the effect of LiBr on the EDLC performance of pectin bio-macromolecular electrolytes is studied and reported by Perumal et al. [134]. They have obtained good window stability of 3.78 V and EDLC is fabricated with the use of activated charcoal-based electrodes. As-fabricated solid-state device exhibits the specific capacitance of 19.04 Fg^{-1} with good reversible performance.
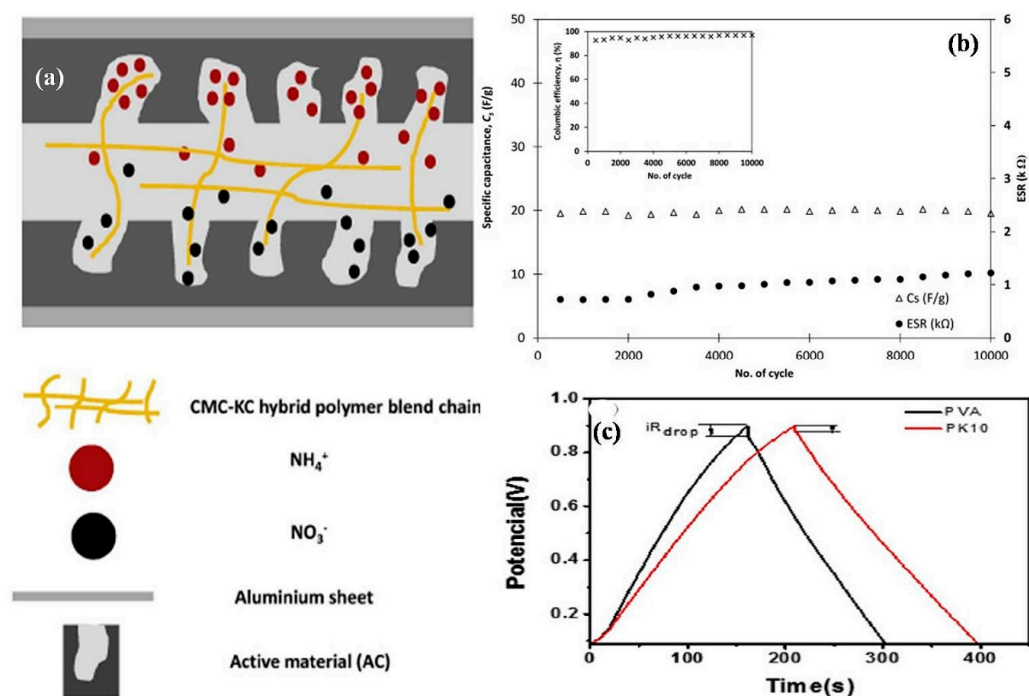

Figure 5. (**a**) Illustration of ion migration at the interface between the HSBEs and electrodes in the EDLC device. (**b**) Specific capacitance (Cs), equivalent series resistant (ESR) and the Columbic efficiency (η%) of the fabricated EDLC device up to the 10,000th cycle (reproduced from Ref. [47] with permission). (**c**) Galvanostatic charge/discharge curves at 0.5 A/g assembled supercapacitor using k-carrageenan electrolytes (reproduced from Ref. [133] with permission).

Hamsan et al. [87] examined the EDLC performance of the prepared potato starch-methyl-cellulose-based blended electrolytes and carbon is used as an electrode material. From the GCD analysis, an initial capacitance of 31 Fg^{-1} is attained. After the multiple cycles, there is a drop in the device capacitance which is due to an increment in the internal resistance of the system and displays the final capacitance of 22 Fg^{-1}. Another survey on the operation of EDLC with the use of plasticized corn starch-based Li-ion conducting electrolytes, was reported by Shukur et al. [86]. The Li-ion conductivity is increased by two orders of magnitude when compared to the un-plasticized sample. The estimated specific capacitance value from the CV measurements and GCD analysis remain the same. Furthermore, the fabricated device reveals a low value of voltage drop, and the value is found to be 0.02–0.04 V. This outcome indicates that the fabricated device holds good

electrode/electrolyte contact and facilitates the higher ionic transportations across the interfacial regime. As a whole, assembled EDLC exhibits a specific capacitance of 33 Fg^{-1} without fading later than 1000 cycles. This type of longer cycling stability is an excellent property for EDLC devices towards the execution of the consumer level.

Important to note that, higher EDLC performance of 133 and 106 Fg^{-1} has been achieved for the plasticized chitosan-starch blended electrolyte with $LiClO_4$ and plasticized poly(styrene sulphonic acid)-starch electrolyte with $LiClO_4$, reported by Sudharkar et al. [135]. On the one hand, nanocomposite cornstarch-based electrolyte records the specific capacitance of 11.11 and 9.83 Fg^{-1} for the $BaTiO_3$ and SiO_2 incorporated samples respectively, examined by Teoh and co-workers [103,104]. More interestingly, ionic liquid added cornstarch and $LiPF_6$ complex reveal the highest EDLC performance of 37 Fg^{-1} investigated by Liew et al. [120]. Natalia H. Wisinka et al. [136] have attempted to prepare polysaccharide-based hydrogels and their electrochemical properties are enriched with the substitution of poly(norepinephrine) towards aqueous capacitor applications. The physicochemical properties of prepared hydrogels are studied by several analytical methods. The well-preserved porosity of the hydrogel is clearly observed from SEM analysis. The electrochemical performance of aqueous capacitors has been studied via different electrolyte systems including acidic (H_2SO_4 and $H_4SiW_{12}O_{40}$), and neutral (Na_2SO_4) systems. Microcrystalline cellulose, agarose, and in situ polymerized norepinephrine (Cel/Aga/p-NBE) hydrogel shows the conductivity and the storage capacitance of 45.9 $mScm^{-1}$, and 127 Fg^{-1} at 0.1 Ag^{-1} respectively. On the other hand, highly flexible cellulose-based hydrogel electrolyte material is studied by Pingxiu Zhang et al. [137]. The quasi-solid-state symmetric configuration of the supercapacitor has been fabricated and achieved an excellent performance of 163.7 Fg^{-1} at 1 Ag^{-1} and capacitance retention of 87.9% is attained after 8k cycles. The electrochemical performance of the assembled supercapacitor has operated at various experimental conditions like different bending angles and lower temperatures. Interestingly, similar storage performance is achieved without loss of capacitance, which indicates that the cellulose hydrogel electrolytes have greater scope in wearable energy devices. Based on these findings, the biopolymer can be recommended to use as a potential electrolyte for solid-state EDLC applications. However, huge variations still exist in the EDLC performance which is mainly derived from the contribution of the various types of electrochemical mechanisms and different host matrixes as well as doped additives. Therefore, more attempts have been required to realize the underlying interfacial electrochemistry and consumer-level execution also.

5.3. Dye-Sensitized Solar Cell

Solar cell technology is considered one of the important alternate renewable energy conversion resources and electricity is generated from direct exposure to the sun. The main obstacle of solar cells is higher cost, which limits their applications in large-scale solar power plants [138]. Therefore, numerous efforts have been paid to search for cost-effective materials without giving up their conductivity. According to their principle, technique, and materials chemistry, solar cells are classified as silicon, quantum dot, CdTe, CdS, perovskite, and DSSC. In this concern, DSSC is a widely adopted technology and utilizes the donor and acceptor nature of organic/inorganic compounds, which leads to form a hetero junction. In DSSC operation, charge generation takes place between the interface of the semiconductor and dye whereas charge transportation occurs via semiconductor/electrolyte. Altering the composition of semiconductor/electrolyte, transportations of mobile carriers are enhanced. Compared to other branches of solar cells, DSSC has additional merits such as a low-cost, sustainable, and simple fabrication process. However, DSSC has some issues like designing the cell, the photodegradation process of used dye and electrode corrosion, etc. So, biopolymer technology has been implemented to resolve the critical problems of DSSC. Typical DSSC contains photoelectrode and a thin layer of conducting oxide-coated counter electrode, which is separated by the redox mediator-assisted electrolytes. The various types of metal oxides/chalcogenides are used as a photoelectrode, which includes TiO_2, SnO_2,

ZrO$_2$, ZnO, Nb$_2$O$_5$, etc. Similarly, several kinds of redox mediators such as thiocyanate, iodide, and cobalt-based mediators are used in the electrolytes. Furthermore, Pt is widely adopted as a counter electrode which is due to the higher value of transmittance, surface area, electrical conductivity, and lesser charge transfer resistance [139,140].

Bella et al. [141] reported the k-carrageenan-based electrolytes for the DSSC analysis. The ionic conductivity of k-carrageenan has been upgraded by the indigenous iodine sublimation process, which may be explained as the incorporation of OH groups with COO$^-$ accordingly increasing the anionic nature of the polymer host. The membrane combination of carboxymethyl k-carrageenan and NaI with 30% EC delivered the utmost conductivity of 5.53×10^{-2} Scm^{-1} along with the sublimation conductivity of 3.25×10^{-3} Scm^{-1}. A solid-state DSSC has been fabricated using the highest conducting electrolyte complex with TiO$_2$ coated FTO—N719 and Pt have been used as photoanode, dye, and counter electrode respectively. Increasing the composition of both NaI and plasticizer, improvement in the short circuit current density as well as efficiency of the assembled device. At the same time, there is no significant difference in the open circuit voltage and fill factor of the device. The obtained maximum efficiency of the solid DSSC is 2.06% and a preliminary stability test was also conducted over the 250 h.

The solid-state DSSC has been assembled with the geometry of FTO-TiO$_2$-N719/carboxyl methyl k-C+ carboxyl methyl cellulose+ 30 wt% NH$_4$I complex/I$_2$-Pt and exhibits the fill factor and energy conversion efficiency of 0.64 and 0.13% respectively. The efficiency of DSSC mainly depends on the open circuit potential, short circuit current, and fill factor. The obtained performance is very low when compared to the earlier surveys and might be due to the poor electrode/electrolyte contact, studied by Rudhziah et al. [142]. In order to improve the electrode/electrolyte interface, various strategies have been performed and all the results are at the pilot level of understanding. In addition to that, understanding of electrode/electrolyte interface is quite different for several electrical devices and needs greater advancements in the characterization techniques for the pre- and post-assembly of the device operation.

On the other hand, CuInS/ZnS quantum dots (QD) and plasticizer incorporated CA-based gel electrolyte shows the highest conductivity of 1.6×10^{-1} Scm^{-1}, studied by Samsi et al. [143]. The reason for conductivity enhancement is due to the interfacial space-charge and percolation model. In other words, added quantum dots are homogeneously distributed in the host matrix resulting in a smoother surface, which leads to improving the interfacial contact. Altering the concentrations of quantum dots, enhancement in the current (J)—voltage (V) response (J$_{sc}$). As an outcome of this, the highest J$_{sc}$ and power conversion efficiency of 11.1 mAcm^{-2} and 8.02% has been attained respectively for the 4 wt% QD assisted sample.

Starch-based 1-methyl-3-propylimidazolium iodide incorporated electrolyte adopted DSSC records the maximum efficiency of 2.09%, which is a much higher value than the other starch-based electrolytes, elucidated by Khanmirzaei et al. [88]. Recently, DSSC has been fabricated using commercial TiO$_2$ paste and records the maximum efficiency of 3.3% and 2.94% for the potato starch nanocrystal gel electrolytes (PNGE) and potato starch gel electrolytes (PGE) respectively, reported by Yogananda et al. [144]. The stability of DSSC was also conducted for the time period of 400 h. The efficiency of the device has been reduced after the 400 h and the value is found to be 2.52% and 2.75% for PGE and PNGE respectively.

Wang and co-workers [145] also implemented the photovoltaic performance of solar devices using highly conducting sodium carboxymethyl starch-based gel electrolytes. Two types of solar cells have been constructed and named: liquid junction quantum dot solar cell (LJQDSC) and quasi solid-state solar cell (QSSSC). They have demonstrated the utmost efficiency of 6.2% and 6.32% for the LJQDSC and QSSSC respectively. Compared to the liquid one, quasi solid-state cells delivered higher efficiency, which may be ascribed to higher ionic conductivity, water uptake, and three-dimensionally conducting porous nature

enabling the rapid transmission of electrons and providing a new research direction to fabricate the quantum dot solar cell.

5.4. Fuel Cell Operations

Nowadays, fuel cell technology has been received as a clean and sustainable source for the generation of electricity among myriad energy conversion devices. Due to the nature of anodes, cathodes, and electrolytes counterparts, fuel cells are widely classified as proton exchange membrane, direct methanol, microbial, and phosphoric fuel cells. Currently, Nafion-based membranes have received commercial benchmark attention, which may be attributed to their excellent chemical stability and higher conductivity. Meanwhile, drawbacks of Nafion membranes are higher cost, difficulty in handling, the higher tendency of permeation, and low thermal and mechanical stability at elevated temperature conditions [146–150]. Hence, cost-effective and mechanically stable alternate membrane research has been prompted all over the globe.

For instance, blend nanocomposite membrane composed of pectin and PVA with the addition of sulphonated TiO_2 as nanofiller, reported by Mohana Priya et al. [149]. Incorporation of nanofiller, the crystallinity percentage of the sample is reduced to the value of 14% when compared to pure PVA and blend samples. Furthermore, an increment in ionic exchange capacity with increasing the S-TiO_2 concentration which can be explained as the addition of an inorganic filler able to separate the hydrophobic and hydrophilic domains. Thus, provides an additional pathway for the proton migration, and leads to higher proton conductivity. In other words, the addition of nanofiller could increase the ionic conductivity via percolating interfacial effect, i.e., anions adsorb on the surface of fillers due to Lewis-acid-base nature, and leads to promote the dissociation of ion pairs, hence enhancement in the conductivity. The maximum proton conducting membrane has been tested for the DMFC operation and shows the power density of 27 mW/cm^2 at a current density of 100 mA/cm^2.

In the same vein, cross-linked and sulphonated alginate and k-carrageenan blended membranes have been tested for DMFC [150]. In the case of acid membranes, ionic conductivity mainly depends on the ionic exchange capacity (IEC) and process of water uptake in which ionic migration involves dissociation of H$^+$ along with water through the Grotthuss and vehicular mechanism. Increasing the carrageenan content, increment in the water uptake and IEC properties thereby assisted the higher proton conductivity. The temperature-dependent DMFC test has been performed using the 80 alginate: 20 k-carrageenan composite membranes and their graph is given in Figure 6a. The obtained open circuit voltage (OCV) is higher than the Nafion membrane and the values are found to be 610, 615, and 625 mV with a maximum power density of 10.4, 13.9, and 17.3 mW/cm^2 at 50, 70, and 90 °C respectively. On the other hand, PEMFC output of 442 and 503 mV has been attained for the iota-Carrageenan doped with NH_4NO_3 and NH_4SCN electrolyte respectively, elucidated by Moniha and co-workers [55,56].

Recently, a CA-based proton conducting membrane has been tested for PEMFC operation and shows the current and power density of 72 mA/cm^2 and 12 mw/cm^2, respectively, studied by Monisha et al. [78]. On the other hand, Tiwari et al. [151,152] studied the effect of salt, solvent, and thickness of the starch membrane on microbial fuel cell applications. The single-channel microbial fuel cell has been constructed using different varieties of prepared membranes. Varying the thickness of the membrane, OCP has been greatly improved and a value of 240 mV is noticed for the salt-added sample. Furthermore, the effect of solvent on the membrane composition records the OCV of 237 mV. Moreover, varying the thickness of the membrane with the presence of salt is essential for a longer lifespan purpose. The same author has studied the proton conducting membrane with varying NaI concentration and maintains the thickness of the film around 4000 microns. Activation energy has been decreased eminently while increasing the content of NaI. The photo snap of the assembled MFC is shown in Figure 6b. The assembled device shows the higher power output, current density, and OCV of 16.68 mWm^{-2}, 85 mAm^{-2}, and 290 mV, respectively.
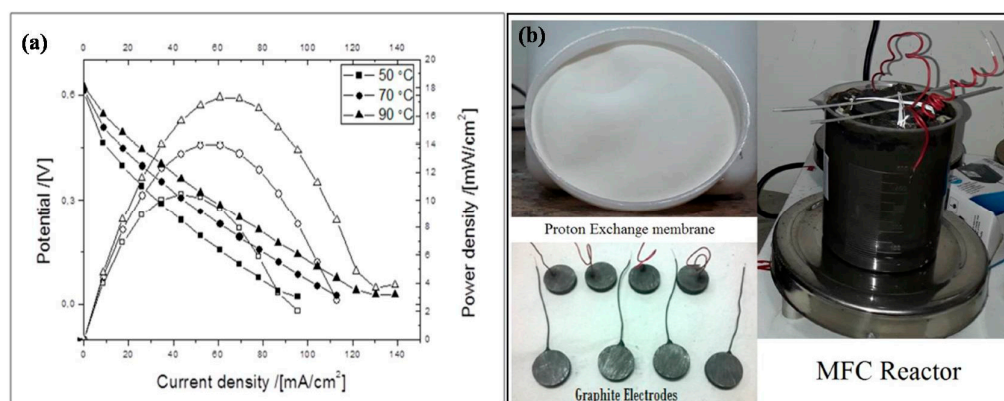
Figure 6. (**a**) I-V curves for DMFC experiments at 50 °C, 70 °C, and 90 °C and 2 M methanol concentration for Alg/Car 80/20 composite membranes. A filled symbol is used for potential and an open symbol for power density (reproduced from Ref. [150] with permission). (**b**) Photograph of prepared membrane, electrode, and MFC reactor (reproduced from Ref. [152] with permission).

6. Summary and Outlook

Polysaccharide-based electrolyte materials have been utilized in various electrical storage/conversion systems and their results are discussed here. Furthermore, this review highlights several promising strategies that have been enabled to enrich the electrochemical performance of the devices. Interestingly, the usage of natural materials not only holds the eco-friendly behavior but also serves as an excellent alternate candidate as the replacement of petroleum-related synthetic host without compromising the adequate characteristics of polymer electrolytes. Notably, a variety of efforts have been made to enhance the biopolymer electrolyte properties via the blending of the host polymer, the introduction of ionic liquids, several metal salts, nanofillers, etc. As an outcome, biopolymer electrolytes exhibit higher ionic conductivity, wider electrochemical stability window, higher transference number, excellent thermal stability, safety, etc. This review article has elaborately discussed conductivity enhancement and the interpretation of results in the most suitable way.

Several ion-conducting electrolytes towards application in flexible/wearable greener electronic gadgets in one review article is an excellent choice and at the same time proves the wider opportunities of biopolymer electrolytes and better knowledge for the readers who might be working in the same general area. In addition, polysaccharide-based materials not only hold the application as an amorphous electrolyte and further extend their application as biomass-derived carbon anode materials for batteries and supercapacitors. Overall, the development of novel electrical conversion and storage devices using polysaccharide-based ion-conducting systems are at the research level of understanding and does not meet any technological breakthroughs. So, further technological implementation is required to promote the commercialization aspect with several parameters have been taken into count. Furthermore, many technical details are needed for the fabrication of the devices via novel designs and fruitful architectures using numerous theoretical models to make an efficient and better understanding of electrical devices.

In addition, challenges and device-level optimization processes co-exist with this thrust area and also the fabrication of the same has varied from device-to-device performances. One of the key challenges is yet to be solved, i.e., poor electrode and solid electrolyte contact which results in higher interfacial resistance. The interfacial problems and interfacial resistance are highly influencing the electrochemical performance, which limits the commercialization of solid-state devices. So, multiple processes are needed to establish efficient interfacial contact via improving the ionic conductivity of the electrolytes of the order of 10^{-1} or 10^{-2} Scm^{-1} and modification of both electrode and electrolyte counterparts. However, the exact electrode/electrolyte interface electrochemistry mechanism is yet to be researched and is in the approximation level of perspective. Analysis of the pre- and post-assembly of the device and in situ characterization techniques will be helpful

to understand the interfacial contact in a better way. As a whole, the implementation of bio-macromolecules in electronic industries has great opportunities to mitigate the potential e-threats as well as promote sustainable and green energy technologies.

Institutional Review Board Statement: Not applicable.

Informed Consent Statement: Not applicable.

Data Availability Statement: Not applicable.

Abbreviations

OCP	Open Circuit Potential
Alutaraldehyde	GA
MIBs	Magnesium Ion Batteries
DMFC	Direct Methanol Fuel Cell
EDLC	Electric Double Layer Capacitor
GCD	Galvanostatic Charging Discharging
IEC	Ionic Exchange Capacity
OCV	Open Circuit Voltage
TSP	Tamarind Seed Polysaccharide
T_g	Glass Transition Temperature
DSSC	Dye-Sensitized Solar Cell
E_a	Activation Energy
EC	Ethylene Carbonate
Mg	Magnesium
i-C	Iota-Carrageenan
K-C	Kappa-Carrageenan
CMC	Carboxymethyl Carrageenan
BmImCl	1-butyl-3-methylimidazolium chloride
SN	Succinonitrile
CA	Cellulose Acetate

References

1. Wang, C.; Wallace, G.G. Flexible electrodes and electrolytes for energy storage. *Electrochim. Acta* **2015**, *175*, 87. [CrossRef]
2. Alipoori, S.; Mazinani, S.; Aboutalebi, S.M.; Sharif, F. Review of PVA-based gel polymer electrolytes in flexible solid-state supercapacitors: Opportunities and challenges. *J. Energy Storag.* **2020**, *27*, 101072. [CrossRef]
3. Perumal, P.; Christopher Selvin, P.; Selvasekarapandian, S.; Sivaraj, P.; Abhilash, K.P.; Moniha, V.; Manjula Devi, R. Plasticizer incorporated, novel eco-friendly bio-polymer based solid bio-membrane for electrochemical clean energy applications. *Polym. Degrad. Stab.* **2019**, *159*, 43. [CrossRef]
4. Guo, T.; Song, J.; Jin, Y.; Sun, Z.; Li, L. Thermally stable and green cellulose-based composites strengthened by styrene-co-acrylate latex for lithium-ion battery separators. *Carbohyd. Polym.* **2019**, *206*, 801. [CrossRef]
5. Arya, A.; Sharma, A.L. Polymer electrolytes for lithium ion batteries: A critical study. *Ionics* **2017**, *23*, 497. [CrossRef]
6. Tan, S.; Zeng, X.; Ma, Q.; Wu, X.; Guo, Y. Recent advancements in polymer-based composite electrolytes for rechargeable lithium batteries. *Electrochem. Energy Rev.* **2018**, *1*, 113. [CrossRef]
7. Kim, J.; Son, B.; Mukherjee, S.; Schuppert, N.; Bates, A.; Kwon, O.; Moon Choi, J.; Chung, H.; Park, S. A review of lithium and non-lithium based solid state batteries. *J. Power Sources* **2015**, *282*, 299. [CrossRef]
8. Sun, C.; Liu, J.; Gong, Y.; Wilkinsone, D.P.; Zhang, J. Recent advances in all-solid-state rechargeable lithium batteries. *Nano Energy* **2017**, *33*, 363. [CrossRef]
9. Dell, R.M. Batteries: Fifty years of materials development. *Solid State Ion.* **2000**, *134*, 139. [CrossRef]
10. Yue, L.; Ma, J.; Zhang, J.; Zhao, J.; Dong, S.; Liu, Z.; Cui, G.; Chen, L. All solid-state polymer electrolytes for high-performance lithium ion batteries. *Energy Storag. Mater.* **2016**, *5*, 139. [CrossRef]
11. Fenton, D.E.; Parker, J.M.; Wright, P.V. Complexes of Alkali Metal Ions with Poly (etylene oxide). *Polymer* **1973**, *14*, 589. [CrossRef]
12. Jabbour, L.; Bongiovanni, R.; Chaussy, D.; Gerbaldi, C.; Beneventi, D. Cellulose-based Li-ion batteries: A review. *Cellulose* **2013**, *20*, 1523. [CrossRef]

13. Singh, R.; Polu, A.R.; Bhattacharya, B.; Rhee, H.; Varlikli, C.; Singh, P.K. Perspectives for solid biopolymer electrolytes in dye sensitized solar cell and battery application. *Renew. Sust. Energ. Rev.* **2016**, *65*, 1098. [CrossRef]

14. Sequeira, C.; Santo, D. *Polymer electrolytes Fundamentals and Applications*; Woodhead Publishing Limited: Sawston, UK, 2010.

15. Mohanty, A.K.; Misra, M.; Drazel, L.T. *Natural Fibers, Biopolymers & Biocomposites*; CRC Press: Boca Raton, FL, USA, 2005.

16. Ngai, K.; Ramesh, S.; Ramesh, K.; Juan, J. A review of polymer electrolytes: Fundamental, approaches and applications. *Ionics* **2016**, *22*, 1259. [CrossRef]

17. Mobarak, N.N.; Ramli, N.; Ahmad, A.; Rahman, M. Chemical interaction and conductivity of carboxymethyl κ-carrageenan based green polymer electrolyte. *Solid State Ion.* **2012**, *224*, 51. [CrossRef]

18. Shamsudin, I.J.; Ahmad, A.; Hassan, N.H.; Kaddami, H. Biopolymer electrolytes based on carboxymethyl ĸ-carrageenan and imidazolium ionic liquid. *Ionics* **2016**, *22*, 841. [CrossRef]

19. Long, L.; Wang, S.; Xiao, M.; Meng, Y. Polymer electrolytes for lithium polymer batteries. *J. Mater. Chem. A* **2016**, *4*, 10038. [CrossRef]

20. Hou, W.; Chen, C.; Wang, C.; Huang, Y. The effect of different lithium salts on conductivity of comb-like polymer electrolyte with chelating functional group. *Electrochim. Acta.* **2003**, *48*, 679. [CrossRef]

21. Aziz, S.B.; Woo, T.J.; Kadir, M.F.Z.; Ahmed, H.M. A conceptual review on polymer electrolytes and ion transport models. *J. Sci. Adv. Mater. Dev.* **2018**, *3*, 1. [CrossRef]

22. Ratner, M.A.; Johansson, P.; Shriver, D.F. Polymer electrolytes: Ionic transport mechanisms and relaxation coupling. *MRS Bull.* **2000**, *25*, 31. [CrossRef]

23. Ratner, M.A.; MacCallum, I.J.R.; Vincent, C.A. *Polymer Electrolytes Reviews*; Elsevier: Amsterdam, The Netherlands, 1987.

24. Willaims, M.L.; Landel, R.F.; Ferry, J.D. The temperature dependence of relaxation mechanisms in amorphous polymers and other glass-forming liquids. *J. Am. Chem. Soc.* **1955**, *77*, 3701. [CrossRef]

25. Ding, L.M.; Shi, J.; Yang, C.Z. Ion-conducting polymers based on modified alternating maleic anhydride copolymer with oligo (oxyethylene) side chains. *Synth. Met.* **1997**, *87*, 157. [CrossRef]

26. Adams, G.; Gibbs, J.H. On the temperature dependence of cooperative relaxation properties in glass-forming liquids. *J. Chem. Phys.* **1965**, *43*, 139. [CrossRef]

27. Shriver, D.F.; Dupon, R.; Stainer, M. Mechanism of ion conduction in alkali metal-polymer complexes. *J. Power Sources* **1983**, *9*, 383. [CrossRef]

28. Druger, S.D.; Ratner, M.A.; Nitzan, A. Generalized hopping model for frequency-dependent transport in a dynamically disordered medium, with applications to polymer solid electrolytes. *Phys. Rev. B* **1985**, *31*, 3939. [CrossRef]

29. Druger, S.D.; Ratner, M.A.; Nitzan, A. Applications of dynamic bond percolation theory to the dielectric response of polymer electrolytes. *Solid State Ion.* **1986**, *18*, 106. [CrossRef]

30. Thakur, B.R.; Singh, R.; Handa, A.K. Chemistry and uses of pectin—A review. *Crit. Rev. Food Sci. Nutr.* **1997**, *37*, 47. [CrossRef]

31. Okenfull, D.G. *The Chemistry of High Methoxyl Pectins in the Chemistry and Technology of Pectin*; Walter, R.H., Ed.; Academic Press: Cambridge, MA, USA, 1991.

32. Andrade, J.; Raphael, E.; Pawlicka, A. Plasticized pectin-based gel electrolytes. *Electrochim. Acta* **2009**, *54*, 6479. [CrossRef]

33. Perumal, P.; Christopher Selvin, P.; Selvasekarapandian, S. Characterization of biopolymer pectin with lithium chloride and its applications to electrochemical devices. *Ionics* **2018**, *24*, 3259. [CrossRef]

34. Perumal, P.; Selvasekarapandian, S.; Abhilash, K.P.; Sivaraj, P.; Hemalatha, R.; Christopher Selvin, P. Impact of lithium chlorate salts on structural and electrical properties of natural polymer electrolytes for all solid state lithium polymer batteries. *Vacuum* **2019**, *159*, 277. [CrossRef]

35. Mishra, R.K.; Anis, A.; Mondal, S.; Dutta, M.; Banthia, A.K. *Chin.* Reparation and characterization of amidated pectin based polymer electrolyte membranes. *J. Polym. Sci.* **2009**, *27*, 639.

36. Muthukrishnan, M.; Shanthi, C.; Selvasekarapandian, S.; Manjuladevi, R.; Perumal, P.; Chrishtopher Selvin, P. Synthesis and characterization of pectin-based biopolymer electrolyte for electrochemical applications. *Ionics* **2019**, *25*, 203. [CrossRef]

37. Kiruthika, S.; Malathi, M.; Selvasekarapandian, S.; Tamilarasan, K.; Moniha, V.; Manjuladevi, R. Eco-friendly biopolymer electrolyte, pectin with magnesium nitrate salt, for application in electrochemical devices. *J. Solid State Electrochem.* **2019**, *23*, 2181. [CrossRef]

38. Kiruthika, S.; Malathi, M.; Selvasekarapandian, S.; Tamilarasan, K.; Maheshwari, T. Conducting biopolymer electrolyte based on pectin with magnesium chloride salt for magnesium battery application. *Polym. Bull.* **2019**, *77*, 6299. [CrossRef]

39. Perumal, P.; Christopher Selvin, P.; Selvasekarapandian, S.; Abhilash, K.P. Bio-host pectin complexed with dilithium borate based solid electrolytes for polymer batteries. *Mater. Res. Exp.* **2019**, *6*, 115513. [CrossRef]

40. Manjuladevi, R.; Christopher Selvin, P.; Selvasekarapandian, S.; Shilpa, R.; Moniha, V. Lithium ion conducting biopolymer electrolyte based on pectin doped with Lithium nitrate. *AIP Conf. Proc.* **2018**, *1942*, 140075.

41. Vijaya, N.; Selvasekarapandian, S.; Sornalatha, M.; Sujithra, K.S.; Monisha, S. Proton-conducting biopolymer electrolytes based on pectin doped with NH_4X (X = Cl, Br). *Ionics* **2016**, *23*, 2799. [CrossRef]

42. Pasini Cabello, S.D.; Ochoa, N.D.; Takara, E.A.; Molla, S.; Compan, V. Influence of Pectin as a green polymer electrolyte on the transport properties of Chitosan-Pectin membranes. *Carbohyd. Polym.* **2017**, *157*, 1759. [CrossRef]

43. Leones, R.; Botelho, M.B.S.; Sentanin, F.; Cesarino, I.; Pawlicka, A.; Camargo, A.S.S.; Silva, M.M. Pectin-based polymer electrolytes with Ir (III) complexes. *Mol. Cryst. Liq. Cryst.* **2014**, *604*, 117. [CrossRef]

44. Masao, K.; Takayuki, H.; Yuuki, K.; Hirohito, U. Solid type dye-sensitized solar cell using polysaccharide containing redox electrolyte solution. *J. Electroanal. Chem.* **2004**, *572*, 21.

45. Liang, L.; Ang, R.N.S.; Mao, S. Carrageenan and its applications in drug delivery. *Carbohyd. Polym.* **2014**, *103*, 1.

46. Campo, V.L.; Kawano, D.F.; da Silva, D.B.; Carvalho, I. Carrageenans: Biological properties, chemical modifications and structural analysis—A review. *Carbohyd. Polym.* **2009**, *77*, 167. [CrossRef]

47. Zainuddin, N.K.; Rasali, N.M.J.; Mazuki, N.F.; Saadiah, M.A.; Samsudin, A.S. Investigation on favourable ionic conduction based on CMC-K carrageenan proton conducting hybrid solid bio-polymer electrolytes for applications in EDLC. *Int. J. Hydrogen Energy* **2020**, *45*, 8727. [CrossRef]

48. Christopher Selvin, P.; Perumal, P.; Selvasekarapandian, S.; Monisha, S.; Boopathi, G.; Leena Chandra, M.V. Study of proton-conducting polymer electrolyte based on K-carrageenan and NH₄SCN for electrochemical devices. *Ionics* **2018**, *24*, 3535. [CrossRef]

49. Mobarak, N.N.; Jumaah, F.N.; Ghani, M.A.; Abdullah, A.; Ahmad, M.P. Carboxymethyl carrageenan based biopolymer electrolytes. *Electrochim. Acta* **2015**, *175*, 224. [CrossRef]

50. Arockia Mary, I.; Selvanayagam, S.; Selvasekarapandian, S.; Srikumar, S.R.; Ponraj, T.; Moniha, V. Lithium ion conducting membrane based on K-carrageenan complexed with lithium bromide and its electrochemical applications. *Ionics* **2019**, *25*, 5839. [CrossRef]

51. Zainuddin, N.K.; Samsudin, A.S. Investigation on the effect of NH4Br at transport properties in k–carrageenan based biopolymer electrolytes via structural and electrical analysis. *Mater. Today Commun.* **2018**, *14*, 199. [CrossRef]

52. Chitra, R.; Sathya, P.; Selvasekarapandian, S.; Monisha, S.; Moniha, V.; Meyvel, S. Synthesis and characterization of iota-carrageenan solid biopolymer electrolytes for electrochemical applications. *Ionics* **2019**, *25*, 2147. [CrossRef]

53. Chitra, R.; Sathya, P.; Selvasekarapandian, S.; Meyvel, S. Synthesis and characterization of iota-carrageenan biopolymer electrolyte with lithium perchlorate and succinonitrile (plasticizer). *Polym. Bull.* **2020**, *77*, 1555. [CrossRef]

54. Karthikeyan, S.; Selvasekarapandian, S.; Premalatha, M.; Monisha, S.; Boopathi, G.; Aristatil, G.; Arun, A.; Madeswaran, S. Proton-conducting I-Carrageenan-based biopolymer electrolyte for fuel cell application. *Ionics* **2017**, *23*, 2775. [CrossRef]

55. Moniha, V.; Alagar, M.; Selvasekarapandian, S.; Sundaresan, B.; Boopathi, G. Conductive bio-polymer electrolyte iota-carrageenan with ammonium nitrate for application in electrochemical devices. *J. Non Cryst. Solids* **2018**, *481*, 424. [CrossRef]

56. Moniha, V.; Alagar, M.; Selvasekarapandian, S.; Sundaresan, B.; Hemalatha, R.; Boopathi, G. Synthesis and characterization of bio-polymer electrolyte based on iota-carrageenan with ammonium thiocyanate and its applications. *J. Solid State Electrochem.* **2018**, *22*, 3209. [CrossRef]

57. Shanmuga Priya, S.; Karthika, M.; Selvasekarapandian, S.; Manjuladevi, R. Preparation and characterization of polymer electrolyte based on biopolymer I-Carrageenan with magnesium nitrate. *Solid State Ion.* **2018**, *327*, 136. [CrossRef]

58. Shanmuga Priya, S.; Karthika, M.; Selvasekarapandian, S.; Manjuladevi, R.; Monisha, S. Study of biopolymer I-carrageenan with magnesium perchlorate. *Ionics* **2018**, *24*, 3861. [CrossRef]

59. Torres, F.G.; Arroyo, J.; Alvarez, R.; Rodriguez, S.; Troncoso, O.; Lopez, D. Carboxymethyl κ/ι-hybrid carrageenan doped with NH₄I as a template for solid bio-electrolytes development. *Mater. Chem. Phys.* **2019**, *223*, 659. [CrossRef]

60. Gidley, M.J.; Lillford, P.J.; Rowlands, D.W.; Lang, P.; Dentini, M.; Crescenzi, V. Structure and solution properties of tamarind-seed polysaccharide. *Carbohyd. Res.* **1991**, *214*, 299. [CrossRef]

61. Premalatha, M.; Mathavan, T.; Selvasekarapandian, S.; Monisha, S.; Vinotpandi, D.; Selvalakshmi, S. Investigations on proton conducting biopolymer membranes based on tamarind seed polysaccharide incorporated with ammonium thiocyanate. *J. Non-Cryst. Solids* **2016**, *453*, 131. [CrossRef]

62. Sharma, M.; Mondal, D.; Mukesh, C.; Prasad, K. Preparation of tamarind gum based soft ion gels having thixotropic properties. *Carbohyd. Polym.* **2014**, *102*, 467. [CrossRef]

63. Van, F.; Lourenco, N.D.; Pinheiro, H.M.; Bakkerd, M. Carrageenan: A food-grade and biocompatible support for immobilisation techniques. *Adv. Synth. Catal.* **2002**, *344*, 815.

64. Sampath Kumar, L.; Christopher Selvin, P.; Selvasekarapandian, S.; Manjuladevi, R.; Monisha, S.; Perumal, P. Tamarind seed polysaccharide biopolymer membrane for lithium-ion conducting battery. *Ionics* **2018**, *24*, 3793. [CrossRef]

65. Agmon, N. The grotthuss mechanism. *Chem. Phys. Lett.* **1995**, *244*, 456. [CrossRef]

66. Kreuer, K.D. Proton conductivity: Materials and applications. *Chem. Mater.* **1996**, *8*, 610. [CrossRef]

67. Gao, H.; Lian, K. Proton-conducting polymer electrolytes and their applications in solid supercapacitors: A review. *RSC Adv.* **2014**, *4*, 33091. [CrossRef]

68. Ndruru, L.; Wahyuningrum, D.; Bundjali, B.; Arcana, M. Preparation and characterization of biopolymer electrolyte membranes based on liclo4-complexed methyl cellulose as lithium-ion battery separator. *J. Eng. Technol. Sci.* **2020**, *52*, 28. [CrossRef]

69. Meyer, W.H. Polymer electrolytes for lithium-ion batteries. *Adv. Mater.* **1998**, *10*, 439. [CrossRef]

70. Sampathkumar, L.; Christopher Selvin, P.; Selvasekarapandian, S.; Perumal, P.; Chitra, R.; Muthukrishnan, M. Synthesis and characterization of biopolymer electrolyte based on tamarind seed polysaccharide, lithium perchlorate and ethylene carbonate for electrochemical applications. *Ionics* **2019**, *25*, 1067. [CrossRef]

71. Perumal, P.; Abhilash, K.P.; Sivaraj, P.; Christopher Selvin, P. Study on Mg-ion conducting solid biopolymer electrolytes based on tamarind seed polysaccharide for magnesium ion batteries. *Mater. Res. Bullet.* **2019**, *118*, 110490. [CrossRef]

72. Premalatha, M.; Mathavan, T.; Selvasekarapandian, S.; Monisha, S.; Selvalakshmi, S.; Vinoth Pandi, D. Tamarind seed polysaccharide (TSP)-based Li-ion conducting membranes. *Ionics* **2017**, *23*, 2677. [CrossRef]

73. Premalatha, M.; Mathavan, T.; Selvasekarapandian, S.; Selvalakshmi, S.; Monisha, S. Development of biopolymer electrolyte membrane using Gellan gum biopolymer incorporated with NH$_4$SCN for electro-chemical application. *Organ Electron.* **2017**, *50*, 418. [CrossRef]

74. Premalatha, M.; Mathavan, T.; Selvasekarapandian, S.; Selvalakshmi, S. Structural and electrical characterization of tamarind seed polysaccharide (TSP) doped with NH$_4$HCO$_2$. *AIP Conf. Proc.* **2018**, *1942*, 70005.

75. Ramesh, S.; Shanti, R.; Morris, E. Plasticizing effect of 1-allyl-3-methylimidazolium chloride in cellulose acetate based polymer electrolytes. *Carbohyd. Polym.* **2012**, *87*, 2624. [CrossRef]

76. Bendaoud, A.; Chalamet, Y. Plasticizing effect of ionic liquid on cellulose acetate obtained by melt processing. *Carbohyd. Polym.* **2014**, *108*, 75. [CrossRef]

77. Monisha, S.; Selvasekarapandian, S.; Mathavan, T.; Milton Franklin Benial, A.; Manoharan, S.; Karthikeyan, S. Preparation and characterization of biopolymer electrolyte based on cellulose acetate for potential applications in energy storage devices. *J. Mater. Sci. Mater. Electron.* **2016**, *27*, 9314. [CrossRef]

78. Monisha, S.; Mathavan, T.; Selvasekarapandian, S.; Milton Franklin Benial, A.; Aristatil, G.; Mani, N.; Premalatha, M.; Vinoth pandi, D. Investigation of bio polymer electrolyte based on cellulose acetate-ammonium nitrate for potential use in electrochemical devices. *Carbohyd. Polym.* **2017**, *157*, 38. [CrossRef]

79. Monisha, S.; Mathavan, T.; Selvasekarapandian, S.; Milton Franklin Benial, A.; Premalatha, M. Preparation and characterization of cellulose acetate and lithium nitrate for advanced electrochemical devices. *Ionics* **2017**, *23*, 2697. [CrossRef]

80. Sudiarti, T.; Wahyuningrum, D.; Bundjali, B.; Made Arcana, I. Mechanical strength and ionic conductivity of polymer electrolyte membranes prepared from cellulose acetate-lithium perchlorate. *IOP Conf. Ser. Mater. Sci. Eng.* **2017**, *223*, 12052. [CrossRef]

81. Lamanna, L.; Pace, G.; Ilic, I.K.; Cataldi, P.; Viola, F.; Friuli, M.; Galli, V.; Demitri, C.; Caironi, M. Edible Cellulose-based Conductive Composites for Triboelectric Nanogenerators and Supercapacitors. *Nano Energy* **2023**, *108*, 108168. [CrossRef]

82. Palanisamy, G.; Oh, T.; Thangarasu, S. Modified Cellulose Proton-Exchange Membranes for Direct Methanol Fuel Cells. *Polymers* **2023**, *15*, 659. [CrossRef]

83. Akhlaq, M.; Mushtaq, U.; Naz, S.; Uroos, M. Carboxymethyl cellulose-based materials as an alternative source for sustainable electrochemical devices: A review. *RSC Adv.* **2023**, *13*, 5723. [CrossRef]

84. Galliard, T. *Starch: Properties and Potentials*; John Wiley & Sons: New York, NY, USA, 1987.

85. Tang, X.; Alavi, S. Recent advances in starch, polyvinyl alcohol based polymer blends, nanocomposites and their biodegradability. *Carbohydr. Polym.* **2011**, *85*, 7. [CrossRef]

86. Shukur, M.F.; Ithnin, R.; Kadir, M.F.Z. Electrical characterization of corn starch-LiOAc electrolytes and application in electrochemical double layer capacitor. *Electrochim. Acta* **2014**, *136*, 204. [CrossRef]

87. Hamsan, M.H.; Shukur, M.F.; Kadir, M.F.Z. NH$_4$NO$_3$ as charge carrier contributor in glycerolized potato starch-methyl cellulose blend-based polymer electrolyte and the application in electrochemical double-layer capacitor. *Ionics* **2017**, *23*, 3429. [CrossRef]

88. Khanmirzaei, M.; Ramesh, S.; Ramesh, K. Polymer electrolyte based dye-sensitized solar cell with rice starch and 1-methyl-3-propylimidazolium iodide ionic liquid. *Mater. Des.* **2015**, *85*, 833. [CrossRef]

89. Yadav, M.; Kumar, M.; Srivastava, N. Supercapacitive performance analysis of low cost and environment friendly potato starch based electrolyte system with anodized aluminium and teflon coated carbon cloth as electrode. *Electrochim. Acta* **2018**, *283*, 1551. [CrossRef]

90. Tiwari, T.; Srivastava, N.; Srivastava, P.C. Ion dynamics study of potato starch+ sodium salts electrolyte system. *Int. J. Electrochem.* **2013**, *2013*, 1. [CrossRef]

91. Khanmirzaei, M.H.; Ramesh, S. Ionic transport and FTIR properties of lithium iodide doped biodegradable rice starch based polymer electrolytes. *Int. J. Electrochem. Sci.* **2013**, *8*, 9977.

92. Hamsan, M.H.; Shukur, M.F.; Kadir, M.F.Z. The effect of NH$_4$NO$_3$ towards the conductivity enhancement and electrical behavior in methyl cellulose-starch blend based ionic conductors. *Ionics* **2017**, *23*, 1137. [CrossRef]

93. Khanmirzaei, M.H.; Ramesh, S.; Ramesh, K. Effect of different iodide salts on ionic conductivity and structural and thermal behavior of rice-starch-based polymer electrolytes for dye-sensitized solar cell application. *Ionics* **2015**, *21*, 2383. [CrossRef]

94. Ahmad Khiar, A.S.; Arof, A.K. Conductivity studies of starch-based polymer electrolytes. *Ionics* **2010**, *16*, 123. [CrossRef]

95. Teoh, K.H.; Lim, C.; Ramesh, S. Lithium ion conduction in corn starch based solid polymer electrolytes. *Measurement* **2014**, *48*, 87. [CrossRef]

96. Tiwari, T.; Pandey, K.; Srivastava, N.; Srivastava, P.C. Effect of glutaraldehyde on electrical properties of arrowroot starch+NaI electrolyte system. *J. Appl. Polym. Sci.* **2011**, *121*, 1. [CrossRef]

97. Tiwari, T.; Srivastava, N.; Srivastava, P.C. Electrical transport study of potato starch-based electrolyte system. *Ionics* **2011**, *17*, 353. [CrossRef]

98. Yadav, M.; Nautiyal, G.; Verma, A.; Kumar, M.; Tiwari, T.; Srivastava, N. Electrochemical characterization of NaClO$_4$–mixed rice starch as a cost-effective and environment-friendly electrolyte. *Ionics* **2019**, *25*, 2693. [CrossRef]

99. Yogananda, K.C.; Ramasamy, E.; Kumar, S.; Vasantha Kumar, S.; Navya Rani, N.; Rangappa, D. Novel rice starch based aqueous gel electrolyte for dye sensitized solar cell application. *Mater. Today Proc.* **2017**, *4*, 12238. [CrossRef]

100. Yusof, Y.M.; Shukur, M.F.; Illias, H.A.; Kadir, M.F.Z. Conductivity and electrical properties of corn starch–chitosan blend biopolymer electrolyte incorporated with ammonium iodide. *Phys. Scr.* **2014**, *89*, 35701. [CrossRef]

101. Bementa, E.; Jothi Rajan, M.A.; Gnanadass, E.S. Effect of prolonged duration of gelatinization in starch and incorporation with potassium iodide on the enhancement of ionic conductivity. *Polym. Plast Technol. Eng.* **2017**, *56*, 1632. [CrossRef]

102. Kulshrestha, N.; Gupta, P.N. Structural and electrical characterizations of 50: 50 PVA: Starch blend complexed with ammonium thiocyanate. *Ionics* **2016**, *22*, 671. [CrossRef]

103. Teoh, K.H.; Lim, C.; Liew, C.; Ramesh, S.; Ramesh, K. Electric double-layer capacitors with corn starch-based biopolymer electrolytes incorporating silica as filler. *Ionics* **2015**, *21*, 2061. [CrossRef]

104. Teoh, K.H.; Lim, C.; Liew, C.; Ramesh, S. Preparation and performance analysis of barium titanate incorporated in corn starch-based polymer electrolytes for electric double layer capacitor application. *J. Appl. Polym. Sci.* **2016**, *133*, 43275. [CrossRef]

105. Amran, N.N.A.; Manan, N.S.A.; Kadir, M.F.Z. The effect of $LiCF_3SO_3$ on the complexation with potato starch-chitosan blend polymer electrolytes. *Ionics* **2016**, *22*, 1647. [CrossRef]

106. Marcondes, R.F.M.S.; D'Agostini, P.S.; Ferreira, J.; Girotto, E.M.; Pawlicka, A.; Dragunski, D.C. Amylopectin-rich starch plasticized with glycerol for polymer electrolyte application. *Solid State Ion.* **2010**, *181*, 586. [CrossRef]

107. Pang, S.; Tay, C.; Chin, S. Starch-based gel electrolyte thin films derived from native sago (Metroxylon sagu) starch. *Ionics* **2014**, *20*, 1455. [CrossRef]

108. Shukur, M.F.; Ibrahim, F.M.; Majid, N.A.; Ithnin, R.; Kadir, M.F.Z. Electrical analysis of amorphous corn starch-based polymer electrolyte membranes doped with LiI. *Phys. Scr.* **2013**, *88*, 25601. [CrossRef]

109. Aziz, S.B.; Asnawi, A.S.F.M.; Mohammed, P.A.; Abdulwahid, R.T.; Yusof, Y.M.; Abdullah, R.M.; Kadir, M.F.Z. Impedance, circuit simulation, transport properties and energy storage behavior of plasticized lithium ion conducting chitosan based polymer electrolytes. *Polym. Test.* **2021**, *101*, 107286. [CrossRef]

110. Shukur, M.F.; Ithnin, R.; Kadir, M.F.Z. Electrical properties of proton conducting solid biopolymer electrolytes based on starch–chitosan blend. *Ionics* **2014**, *20*, 977. [CrossRef]

111. Shukur, M.F.; Kadir, M.F.Z. Hydrogen ion conducting starch-chitosan blend based electrolyte for application in electrochemical devices. *Electrochim. Acta* **2015**, *158*, 152. [CrossRef]

112. Shukur, M.F.; Kadir, M.F.Z. Electrical and transport properties of NH_4Br-doped cornstarch-based solid biopolymer electrolyte. *Ionics* **2015**, *21*, 111. [CrossRef]

113. Yusof, Y.M.; Majid, N.A.; Kasmani, R.M.; Illias, H.A.; Kadir, M.F.Z. The effect of plasticization on conductivity and other properties of starch/chitosan blend biopolymer electrolyte incorporated with ammonium iodide. *Mol. Cryst. Liq. Cryst.* **2014**, *603*, 73. [CrossRef]

114. Hamsan, M.H.; Aziz, S.B.; Shukur, M.F.; Kadir, M.F.Z. Protonic cell performance employing electrolytes based on plasticized methylcellulose-potato starch-NH_4NO_3. *Ionics* **2019**, *25*, 559. [CrossRef]

115. Yusof, Y.M.; Kadir, M.F.Z. Electrochemical characterizations and the effect of glycerol in biopolymer electrolytes based on methylcellulose-potato starch blend. *Mol. Cryst. Liq. Cryst.* **2016**, *627*, 220. [CrossRef]

116. Yusof, Y.M.; Illias, H.A.; Shukur, M.F.; Kadir, M.F.Z. Characterization of starch-chitosan blend-based electrolyte doped with ammonium iodide for application in proton batteries. *Ionics* **2017**, *23*, 681. [CrossRef]

117. Shukur, M.F.; Majid, N.A.; Ithnin, R.; Kadir, M.F.Z. Effect of plasticization on the conductivity and dielectric properties of starch–chitosan blend biopolymer electrolytes infused with NH_4Br. *Phys. Scr.* **2013**, *T157*, 14051. [CrossRef]

118. Shukur, M.F.; Ithnin, R.; Kadir, M.F.Z. Protonic transport analysis of starch-chitosan blend based electrolytes and application in electrochemical device. *Mol. Cryst. Liq. Cryst.* **2014**, *603*, 52. [CrossRef]

119. Khanmirzaei, M.H.; Ramesh, S. Nanocomposite polymer electrolyte based on rice starch/ionic liquid/TiO_2 nanoparticles for solar cell application. *Measurement* **2014**, *58*, 68. [CrossRef]

120. Liew, C.; Ramesh, S. Electrical, structural, thermal and electrochemical properties of corn starch-based biopolymer electrolytes. *Carbohyd. Polym.* **2015**, *124*, 222. [CrossRef]

121. Liew, C.; Ramesh, S. Studies on ionic liquid-based corn starch biopolymer electrolytes coupling with high ionic transport number. *Cellulose* **2013**, *20*, 3227. [CrossRef]

122. Ramesh, S.; Shanti, R.; Morris, E. Studies on the plasticization efficiency of deep eutectic solvent in suppressing the crystallinity of corn starch based polymer electrolytes. *Carbohyd. Polym.* **2012**, *87*, 701. [CrossRef]

123. Shukur, M.F.; Ithnin, R.; Kadir, M.F.Z. Ionic conductivity and dielectric properties of potato starch-magnesium acetate biopolymer electrolytes: The effect of glycerol and 1-butyl-3-methylimidazolium chloride. *Ionics* **2016**, *22*, 1113. [CrossRef]

124. Azli, A.A.; Manan, N.S.A.; Kadir, M.F.Z. The development of Li+ conducting polymer electrolyte based on potato starch/graphene oxide blend. *Ionics* **2017**, *23*, 411. [CrossRef]

125. Ramesh, S.; Shanti, R.; Morris, E.; Durairaj, R. Utilisation of corn starch in production of 'green'polymer electrolytes. *Mater. Res. Innov.* **2011**, *15*, 8. [CrossRef]

126. Huang, Y.; Liu, J.; Zhang, J.; Jin, S.; Jiang, Y.; Zhang, S.; Li, Z.; Zhi, C.; Due, G.; Zhou, H. Flexible quasi-solid-state zinc ion batteries enabled by highly conductive carrageenan bio-polymer electrolyte. *RSC Adv.* **2019**, *9*, 16313. [CrossRef]

127. Leng, L.; Zeng, X.; Chen, P.; Shu, T.; Song, H.; Fu, Z.; Wang, H.; Liao, S. A novel stability-enhanced lithium-oxygen battery with cellulose-based composite polymer gel as the electrolyte. *Electrochim. Acta* **2015**, *176*, 1108. [CrossRef]

128. Liu, J.; Li, W.; Zuo, X.; Liu, S.; Li, Z. Polyethylene-supported polyvinylidene fluoride–cellulose acetate butyrate blended polymer electrolyte for lithium ion battery. *J. Power Sources* **2013**, *226*, 101. [CrossRef]

129. Nirmale, T.C.; Karbhal, I.; Kalubarme, R.S.; Shelke, M.V.; Varma, A.J.; Kale, B.B. Facile synthesis of unique cellulose triacetate based flexible and high performance gel polymer electrolyte for lithium ion batteries. *ACS Appl. Mater. Interfaces* **2017**, *9*, 34773. [CrossRef]

130. Zhao, M.; Zuo, X.; Wang, C.; Xiao, X.; Liu, J.; Nan, J. Preparation and performance of the polyethylene-supported polyvinylidene fluoride/cellulose acetate butyrate/nano-SiO$_2$ particles blended gel polymer electrolyte. *Ionics* **2016**, *22*, 2123. [CrossRef]

131. Lin, Y.; Li, J.; Liu, K.; Liu, Y.; Liu, J.; Wang, X. Unique starch polymer electrolyte for high capacity all-solid-state lithium sulfur battery. *Green Chem.* **2016**, *18*, 3796. [CrossRef]

132. Zhong, C.; Deng, Y.; Hu, W.; Qiao, J.; Zhang, L.; Zhang, J. A review of electrolyte materials and compositions for electrochemical supercapacitors. J. *Chem. Soc. Rev.* **2015**, *44*, 7484. [CrossRef]

133. Hu, X.; Fan, L.; Qin, G.; Shen, Z.; Chen, J.; Wang, M.; Yang, J.; Chen, Q. Flexible and low temperature resistant double network alkaline gel polymer electrolyte with dual-role KOH for supercapacitor. *J. Power Sources* **2019**, *414*, 201. [CrossRef]

134. Perumal, P.; Christopher Selvin, P. Boosting the performance of electric double layer capacitor via engaging pectin macromolecular electrolyte with elevated ionic conductivity and potential window stability. *Chem. Eng. J. Adv.* **2021**, *8*, 100178. [CrossRef]

135. Sudhakar, Y.N.; Selvakumar, M. Ionic conductivity studies and dielectric studies of poly (styrene sulphonic acid)/starch blend polymer electrolyte containing LiClO$_4$. *J. Appl. Electrochem.* **2013**, *43*, 21. [CrossRef]

136. Wisinska, N.H.; Skunik-Nuckowska, M.; Garbacz, P.; Dyjak, S.; Wieczorek, W.; Kulesza, P.J. Polysaccharide-based hydrogel electrolytes enriched with poly (norepinephrine) for sustainable aqueous electrochemical capacitors. *J. Environ. Chem. Eng.* **2023**, *11*, 109346. [CrossRef]

137. Zhang, P.; Li, M.; Jing, Y.; Zhang, X.; Su, S.; Zhu, J.; Yu, N. Highly flexible cellulose-based hydrogel electrolytes: Preparation and application in quasi solid-state supercapacitors with high specific capacitance. *J. Mater. Sci.* **2023**, *58*, 1694. [CrossRef]

138. Agiorgousis, M.L.; Sun, Y.; Zeng, H.; Zhang, S. Strong covalency-induced recombination centers in perovskite solar cell material CH$_3$NH$_3$PbI$_3$. *J. Am. Chem. Soc.* **2014**, *136*, 14570. [CrossRef] [PubMed]

139. Suait, M.S.; Rahman, M.Y.A.; Ahmad, A. Review on polymer electrolyte in dye-sensitized solar cells (DSSCs). *Sol. Energy* **2015**, *115*, 452. [CrossRef]

140. Wang, W.; Zhuo, S.; Wang, L.; Fang, S.; Lin, Y. Mono-ion transport electrolyte based on ionic liquid polymer for all-solid-state dye-sensitized solar cells. *Sol. Energy* **2012**, *86*, 1546. [CrossRef]

141. Federico Bella Nadhratun, N.; Mobarak Fatihah, N.; Ahmad, A. From seaweeds to biopolymeric electrolytes for third generation solar cells: An intriguing approach. *Electrochim. Acta* **2015**, *151*, 306.

142. Rudhziah, S.; Ahmad, A.; Ahmad, I.; Mohamed, N.S. Biopolymer electrolytes based on blend of kappa-carrageenan and cellulose derivatives for potential application in dye sensitized solar cell. *Electrochim. Acta* **2015**, *175*, 162. [CrossRef]

143. Samsi, N.S.; Effendi, N.F.S.; Zakaria, R.; Ali, A.M.M. Efficiency enhancement of dye-sensitized solar cell utilizing copper indium sulphide/zinc sulphide quantum dot plasticized cellulose acetate polymer electrolyte. *Mater. Res. Express* **2017**, *4*, 44005. [CrossRef]

144. Yogananda, K.C.; Ramasamy, E.; Vasantha Kumar, S.; Rangappa, D. Synthesis, characterization, and dye-sensitized solar cell fabrication using potato starch–and potato starch nanocrystal–based gel electrolytes. *Ionics* **2019**, *25*, 6035. [CrossRef]

145. Wang, X.; Feng, W.; Wang, W.; Wang, W.; Zhao, L.; Li, Y. Sodium carboxymethyl starch-based highly conductive gel electrolyte for quasi-solid-state quantum dot-sensitized solar cells. *Res. Chem. Intermed.* **2018**, *44*, 1161. [CrossRef]

146. Hanif, M.B.; Motola, M.; Qayyum, S.; Rauf, S.; Khalid, A.; Li, C.; Li, X. Recent advancements, doping strategies and the future perspective of perovskite-based solid oxide fuel cells for energy conversion. *Chem. Eng. J.* **2022**, *428*, 132603. [CrossRef]

147. Rauf, S.; Hanif, M.; Wali, M.; Tayyab, Z.; Zhu, B.; Mushtaq, N.; Yang, Y.; Khan, K.; Lund, P.; Martin, M.; et al. Highly active interfacial sites in SFT-SnO$_2$ heterojunction electrolyte for enhanced fuel cell performance via engineered energy bands: Envisioned theoretically and experimentally. *Energy Environ. Mater.* **2023**, e12606. [CrossRef]

148. Hanif, M.B.; Rauf, S.; Mosiałek, M.; Khan, K.; Kavaliukė, V.; Kežionis, A.; Šalkus, T.; Gurgul, J.; Medvedev, D.; Zimowska, M.; et al. Mo-doped BaCe$_{0.9}$Y$_{0.1}$O$_{3-\delta}$ proton-conducting electrolyte at intermediate temperature SOFCs. Part I: Microstructure and electrochemical properties. *Int. J. Hydrogen Energy*, 2023; *in press*. [CrossRef]

149. Mohanapriya, S.; Rambabu, G.; Bhat, G.D.; Raj, V. Pectin based nanocomposite membranes as green electrolytes for direct methanol fuel cells. *Arab. J. Chem.* **2020**, *13*, 2024. [CrossRef]

150. Pasini Cabello, S.D.; Mollá, S.; Ochoa, N.A.; Marchese, J.; Giménez, G.; Compan, V. New bio-polymeric membranes composed of alginate-carrageenan to be applied as polymer electrolyte membranes for DMFC. *J. Power Sources* **2014**, *265*, 345. [CrossRef]

151. Tiwari, T.; Srivastava, N. Exploring the Possibility of Starch-Based Electrolyte Membrane in MFC Application. *Macromol. Symp.* **2019**, *388*, 1900041. [CrossRef]

152. Tiwari, T.; Kumar, M.; Yadav, M.; Srivastava, N. Study of Arrowroot Starch-Based Polymer Electrolytes and Its Application in MFC. *Starch Stärke* **2019**, *71*, 1800313. [CrossRef]